Spatio-temporal dynamics of word retrieval in speech production revealed by cortical high frequency band activity

Stephanie K. Riès[1,2], Rummit K. Dhillon[2], Alex Clarke[3,4], David King-Stephens[3], Kenneth D. Laxer[5,7], Peter B. Weber[5], Rachel A. Kuperman[6], Kurtis I. Auguste[6,7], Peter Brunner[8], Gerwin Schalk[8], Jack J. Lin[9], Josef Parvizi[10], Nathan E. Crone[11], Nina F. Dronkers[3,12], and Robert T. Knight[2]

1. School of Speech, Language, and Hearing Sciences, San Diego State University, 5500 Campanile Dr, San Diego, CA 92182, USA.
2. Helen Wills Neuroscience Institute and Department of Psychology, 132 Barker Hall, University of California, Berkeley, CA 94720-3190, USA.
3. University of California Davis Center for Neuroscience, 1544 Newton Court, Davis, CA 95618, USA.
4. Department of Psychology, University of Cambridge, Cambridge, CB2 3EB, United Knigdom.
5. California Pacific Medical Center, 2100 Webster Street, San Francisco, CA 94115, USA.
6. Children's Hospital and Research Center, Oakland, CA, USA
7. University of California San Francisco Medical Center, 505 Parnassus Ave, San Francisco, CA 94143, USA.
8. New York State Department of Health, Wadsworth Center, and Department of Neurology, Center for Medical Science, 150 New Scotland Ave., Albany, NY 12208, Albany, NY, USA.
9. Department of Neurology, School of Medicine, University of California, 105 Irvine Hall, Irvine, CA 92697, USA.
10. Stanford Human Intracranial Cognitive Electrophysiology Program (SHICEP), Stanford University, 300 Pasteur Dr, Stanford, CA 94305, USA.
11. Department of Neurology, The Johns Hopkins University School of Medicine, 600 N Wolfe St # 2147, Baltimore, MD 21287, USA.
12. Center for Aphasia & Related Disorders, Veterans Affairs Northern California Health Care System. 150 Muir road 126S, Martinez, CA 94553, USA.

Corresponding author:

Stephanie Ries, PhD
School of Speech, Language, and Hearing Sciences
San Diego State University
5500 Campanile Dr
San Diego, CA 92182, USA.
telephone: 619-594-2373
email: sries@sdsu.edu

Keywords:

word retrieval, language production, electrocorticography, lexical activation, word selection, cortical high-gamma.

Abstract

Word retrieval is core to language production and relies on two complementary processes: rapid lexical-semantic activation, and word selection which chooses the correct word among semantically-related competitors. Lexical-semantic activation is measured by semantic priming. In contrast, word selection is indexed by semantic interference and is hampered in semantically-homogeneous contexts. We examined the spatiotemporal dynamics of these two complimentary processes in a picture naming task with blocks of semantically heterogeneous (HET) or homogeneous (HOM) stimuli. We used electrocorticography data obtained from frontal and temporal cortices permitting detailed spatio-temporal analysis of both lexical-semantic activation and word selection. A semantic interference effect was observed with naming latencies longer in HOM versus HET blocks. Cortical response strength as indexed by high frequency band activity (HFB, 70-150 Hz) amplitude revealed effects linked to both lexical-semantic activation and word selection. Depending on the sub-second timing and cortical region, HFB showed either semantic interference (more activity in HOM than HET blocks), or semantic priming effects (more activity in HET than HOM blocks). These effects overlapped in time and space in the left posterior inferior temporal gyrus and the left prefrontal cortex. This data does not support a strict modular view of word retrieval in speech production but rather support substantial overlap of lexical-semantic activation and word selection mechanisms in the brain.

Significance

Word retrieval is essential to language production relying on activation of word representations in memory followed by selection of the correct word. The detailed spatio-temporal cortical dynamics of this core language process are not well-known. Using direct cortical recordings we show that the activation of word representations and their selection co-occur in time and engage overlapping brain regions. In contrast with present modular brain models of language production, our data do not support a clear division of labor between brain regions during lexical-semantic activation and word selection. We suggest that overlapping brain mechanisms optimize word retrieval.

\body

Introduction

Adults fluidly utter 2 to 3 words per second selected from up to 100,000 regularly-used words in the mental lexicon (1). Word retrieval accesses and fits an appropriate word to ongoing speech and is core to language production as evidenced by the severe impact of word retrieval deficits, such as anomia[1]. Despite the importance of word retrieval in language and the immense personal and societal cost caused by its disruption in neurological disorders, its neural basis is poorly understood. The present study sheds light on the spatio-temporal dynamics of word activation and selection at the sub-second scale using direct cortical recordings in neurosurgical patients.

Word retrieval is enabled through two complementary processes: rapid lexical-semantic activation, and word selection, identifying the correct word among semantically-related competitors. Lexical-semantic activation is indexed by semantic priming, wherein a prior semantically related word leads to more rapid word identification, an effect that has been reported during both language comprehension (3) and language production (4). Word selection is indexed by the opposite effect referred to as semantic interference. Word selection is hampered in semantically homogeneous contexts, where the presence of semantic competitors is high (for a discussion of the competitive vs. non-competitive nature of lexical selection see (4-6). Whereas in some models word selection occurs through internal dynamics of lexical representations (7), others suggest an external mechanism acts upon the activation of lexical representations to select the correct candidate word (e.g., 8,9). In this study, we test whether the external selection module suggested by this second class of models is hosted by brain regions different from those engaged in initial lexico-semantic activation. The blocked-cyclic picture naming paradigm (10) is widely utilized to study the cognitive and neurological correlates of word retrieval (e.g., 11-16). In this paradigm, pictures are presented one by one in semantically-homogeneous (HOM, all pictures are from the same semantic category) or heterogeneous blocks (HET, all pictures are from different semantic categories). The pictures are repeated several times per block (typically between 4 and 6 times), leading to a main repetition priming effect (4,5). Performance as assessed with naming latencies and error rates is typically worse in HOM than in HET blocks from the 2nd cycle onward. Thus, in HOM blocks, repetition priming is countered by a semantic interference effect indexing word selection difficulty, which is increased when semantically-related competitors receive additional activation.

A fronto-temporal network of brain regions has been associated with word retrieval. In particular, the left inferior frontal gyrus (LIFG) has been associated with word selection. This region has been described as

1

Anomia is a severe word retrieval deficit observed in all aphasic patients as well as in neurodegenerative diseases and normal aging (2).

providing top-down control to help overcome interference caused by semantically-related alternatives (12,13), thus hosting the external selection above-mentioned module (9). Medial frontal regions such as the pre-supplementary motor area (pre-SMA) and the anterior cingulate cortex (ACC) have also been associated with response selection in and outside the field of language production (17-19). The left posterior temporal regions including the middle temporal gyrus (MTG) (20) and the inferior temporal gyrus (ITG) (21) have been proposed to play a central role in word retrieval. Most reports focus on word selection, as indexed by semantic interference (i.e., more activity in HOM versus HET contexts). Interestingly however, some fMRI (19,22), but also MEG (14,23), and EEG picture naming studies of word retrieval (15,16) have shown that the reverse effect, semantic facilitation or priming, is also observed using paradigms eliciting semantic interference effects on reaction times. This effect is manifested by early increased activation in HET blocks than HOM blocks, reflecting poorer lexical-semantic priming in HET than HOM blocks. This suggests that signatures of lexical-semantic activation in speech production can be observed even when the main behavioral effect is in the opposite direction. The cortical spatio-temporal interplay of lexical-semantic activation and word selection is unclear but recent studies have suggested a fronto-temporal division of labor where the left temporal lobe would be predominantly involved in supporting lexical-semantic activation and the frontal lobe would support top-down control processes narrowing the search for the target word (19,23). In the present study, we address the precise spatio-temporal network underlying word retrieval in speech production in the human brain using direct cortical recordings in neurosurgical patients, offering millisecond- and centimeter-scale resolution. Recent intracranial EEG studies have provided rare insight into the spatio-temporal dynamics of speech production (24,25) and the speech output stages in the motor and sensory cortices (26), but none have focused on the cortical spatio-temporal dynamics of word retrieval (see however (27-29 for hippocampal word-retrieval related activity). In the present study, we used the blocked-cyclic picture naming paradigm, a psycholinguistic task specifically tailored to focus on word retrieval processes in language production. We provide new insights into the spatio-temporal dynamics of lexical-semantic activation and word selection in word retrieval during speech production.

Results

Patients and Behavior

Nine patients participated in the study, including 7 with left hemisphere coverage (Figure S1). Here we report effects of Semantic Context and its interaction with other factors under analysis. Other effects not involving Semantic Context are reported in the supporting information. The electrophysiological data analysis was focused on left hemisphere regions previously associated with word retrieval. The 2 patients with right hemisphere coverage had minimal coverage over the lateral frontal, medial frontal and posterior temporal cortices (see Figure S5 for an overview of the semantic context effects per electrode in the right hemisphere stimulus- and response-locked).

Of the 7 patients with left hemisphere coverage, one patient (IR02, in orange on Figure S1), whose seizure focus was in the posterior medial PFC (in the pre-SMA area, Figure S2 shows the resected area), had poor performance (error rate > 40%) in this task and his behavioral and ECoG data were analyzed separately. His semantic interference effect on naming latencies (321 ms) was more than 3 standard deviations larger than that of the other patients (mean = 43 ms, SD = 82 ms). This case study indicates that, when brain tissue in the posterior medial PFC is abnormal, interference caused by semantically-related alternatives is more difficult to overcome.

In the remaining 8 patients, we found the expected pattern of results in the behavioral data (mean naming latencies and standard deviations per semantic context and per presentation number are presented in Figure 1A and Table S1 in SI). Because the semantic interference effect can be absent or even reversed in the first presentation and because performance is more variable in this first cycle (30,31), we performed the analysis without the first presentation of the stimuli (as in ([13,32] but see SI for an analysis including presentation 1). There was a main effect of Semantic Context on log-transformed[2] naming latencies (*Wald* $\chi^2(1) = 4.82$, $p = .028$): participants were slower in HOM vs. HET blocks, revealing a semantic interference effect (see Table S2 A for β_{raw}, CI, SE, and t-values). Finally, there was an interaction between Semantic Context and Presentation Number (*Wald* $\chi^2(1) = 6.38$, $p = .012$): with increasing repetitions, naming latencies increased in HOM vs. HET blocks. The error-rate was overall low (median = 3.64%, IQR (Inter-quartile range) = [1.82-8.85]), and there was no significant effect of any of the experimental parameters we controlled for on accuracy rates when the 1st presentation of the stimuli was removed (see SI, and Figure 1B for details).

Electrocorticography

We focused our electrophysiological analysis on high frequency band activity (HFB, 70-150 Hz) as HFB power has been found to be the most reliable spectral measure of cortical activation in language production

---

2 The individual reaction times (RTs) were log-transformed to reduce skewness and approach a normal distribution.

tasks (24,25), and is the most commonly used spectral profile in intracranial language research (33). In addition, HFB is ubiquitous in the human cortex is known to be a robust correlate of local neuronal activation, and is reliable on a single-trial basis (34,35)[3]. We first examined the presence of HFB in each electrode in 1000-ms stimulus and response-locked time windows (see Methods and Figure S3). Out of the 617 artifact and seizure-free electrodes across patients, 304 had significant HFB time-locked to the stimulus (median: 37 electrodes per patient, IQR = [31-46]), and 307 had significant HFB time-locked to vocal-onset (median: 37 electrodes per patient, IQR = [34-39]) (Figure S4). Thus, a median of 49 % of included electrodes were task-active electrodes stimulus-locked (IQR = [48-53]), and a median of 51 % of included electrodes were task-active electrodes response-locked (IQR = [46-58]). Active electrodes were observed in all cortical lobes. The analyses of experimental effects were carried out on these active electrodes in the frontal and temporal lobes. We used linear mixed effects models to analyze how HFB amplitude was modulated by Semantic Context and its interaction with the other factors. These included, presentation number, stimulus position, cortical Structure[4], and time-Window (i.e., divided in five 200-ms chunks stimulus and response-locked), in the left frontal and temporal cortices in the 6 patients with normal language production (see Methods).

Stimulus-locked semantic context effects

In the stimulus-locked analyses, Semantic Context effects were found in both the temporal and frontal lobe models. The distribution of raw β weights per Window on the left lateral surface for the semantic context effects stimulus-locked are presented in Figure 2A.

In the temporal lobe, Semantic Context interacted with Window (*Wald* $\chi^2(1) = 7.75$, p = .005): semantic interference increased the further away from stimulus onset (see Figure 3A and Table S4). There was also a 3-way interaction between Semantic Context, Window, and Structure (*Wald* $\chi^2(3) = 11.23$, p = .011), indicating the semantic interference effect increased only in the ITG whereas the semantic priming effect increased in the other structures (MTG vs. ITG: β_{raw}=-1.57; CI= [-2.592 -5.59 x 10^{-1}], SE= 5.18 x 10^{-1}, t=-3.04; STG vs. ITG: β_{raw}=-1.60; CI= [-2.63 -5.78 x 10^{-1}], SE= 5.23 x 10^{-1}, t=-3.03; Ventral vs. ITG: β_{raw}=-8.84 x 10^{-1}; CI= [-2.23 4.63 x 10^{-1}], SE= 6.72 x 10^{-1}, t=-1.29). This explains the absence of an overall main

---

3 Because most scalp EEG studies using this paradigm have focused on event-related potentials, we also conducted an analysis of the intracranial ERPs recorded across ECoG recording sites. Several studies have shown that ERPs described at the scalp surface are often associated with more than one cortical generator (e.g., 36-39). In addition, intracranial ERPs are found at recording sites which do not necessarily overlap with those at which HG is recorded (39,40). In our study, this was also the case, there was only about 40% overlap in the sites showing HG and those showing ERPs. In addition, almost no significant semantic context effects were found in the ERP analysis (see SI for more details).

4 Four structures per lobe were defined: In the frontal cortex, lateral prefrontal cortex (PFC), medial PFC, lateral primary motor cortex and pre-motor cortex (lateral M1/PMC), and medial M1/PMC. In the temporal cortex, lateral superior temporal gyrus (STG), middle temporal gyrus (MTG), and inferior temporal gyrus (ITG), and ventral temporal cortex.

effect of Semantic Context (*Wald* $\chi^2(1) = 2.19$, p = .139) in the temporal lobe. The semantic interference effect in the ITG emerged in the 400 ms to 600 ms time-window after stimulus onset, similar to that observed in the frontal lobe (see Fig 4A). Before that time window, the dominant effect in this brain region was semantic priming (this was observed for 3 patients out of 4 having electrode coverage in the ITG, Figure S6A). This suggests that this region is initially involved in lexical-semantic activation followed by word selection, indicating the same brain region may be involved in these two complementary processes supporting word retrieval at different time points.

In the frontal lobe, there was a marginal Semantic Context effect (*Wald* $\chi^2(1) = 3.21$, p = .073) and an interaction between Semantic Context and Window (*Wald* $\chi^2(1) = 4.54$, p = .033) (see Figure 3A and Table S3 for statistical details). Importantly, the direction of the evolution of the semantic context effect depended on the region of the frontal cortex involved. There was a 3-way interaction between Semantic Context, Window, and Structure (*Wald* $\chi^2(3) = 8.96$, p = .030). In the lateral PFC and medial M1/PMC in comparison with the lateral M1/PMC, semantic interference tended to increase with time (lateral PFC vs. lateral M1/PMC: $\beta_{raw}=6.09 \times 10^{-1}$; CI= [0.05 1.16], SE= 2.83×10^{-1}, t=2.15; medial M1/PMC vs. lateral M1/PMC: $\beta_{raw}=8.31 \times 10^{-1}$; CI= [-0.13 1.80], SE= 4.92×10^{-1}, t=1.69). There was no significant difference in the direction of the interaction between the lateral M1/PMC and the medial PFC (Table S3). Semantic Context did not interact with any of the other factors analyzed. These results underlie the role of the lateral PFC and medial M1/PMC in semantic interference resolution for word selection starting around 400 ms post-stimulus onset.

We also found substantial temporal overlap between the semantic interference and priming effects in the temporal and frontal lobes. Indeed, while semantic interference increased in the ITG, lateral PFC, and medial M1/PMC, semantic priming increased in the other structures (as reported above and in Tables S3 and S4). There was no significant difference between the time-windows in which the maximal semantic interference effect was reached in the ITG, lateral PFC, and medial M1/PMC compared to when the maximal priming effect was reached in the other structures (t(20.78)=.85, p=.405; on average between 600 and 800 ms after stimulus onset). This observation is in agreement with substantial temporal overlap between the two processes, in agreement with models allowing some degree of interaction between lexical-semantic activation and word selection brain regions (e.g., 41,8).

Response-locked semantic context effects

Response-locked effects of Semantic Context were clearer in the frontal than in the temporal lobe models (Figure 2B).

In the temporal lobe, there was no main effect of Semantic Context response-locked (*Wald* $\chi^2(1) = 2.11$, p = .146), nor any 2 or 3-way interaction of Semantic Context with any of the other factors under analysis (see Table S6 for statistical details). The observation that semantic context effects were not as clear for response-locked compared to stimulus-locked in the temporal lobe suggests that temporal lobe regions, and especially the ITG, is engaged in word retrieval in a stimulus-bound manner.

In the frontal lobe, there was a main effect of Semantic Context (*Wald* $\chi^2(1) = 6.45$, p = .011): there was more HFB in HOM than HET blocks in all of the frontal structures under analysis (see Figure 3B and Table S5). Thus, the response-locked effects of Semantic Context were clearer than the stimulus-locked ones in the frontal lobe. This suggests a sustained involvement of the PFC in semantic interference resolution. In addition, semantic interference decreased the closer to vocal onset as indicated by an interaction between Semantic Context and Window (*Wald* $\chi^2(1) = 4.47$, p = .03). As can be seen on the by-patient averages, semantic interference was present until around 350 ms prior to vocal onset.

The stimulus-bound engagement of the temporal cortex therefore contrasts with the more sustained involvement of the PFC and underlies the different roles of these brain regions in word retrieval.

HFB-RT correlations

These results do not take into account how cortical response strength relates to trial-by-trial performance in these regions during word retrieval. To address this, we examined how within-trial mean HFB for stimulus and response-locked time windows correlated with reaction times as measured with naming latencies. We calculated Spearman rank correlation tests at each electrode site (rho correlation coefficient per time-window and per electrode stimulus and response-locked shown in Figure S7, see SI for methods).

As was clearly visible in the response-locked analysis of the frontal lobe data, structures showing semantic interference in given time-windows showed predominantly positive HFB-RT correlations, where higher within-trial mean HFB values were associated with longer RTs, in the same time-windows (Figure 4B). HFB-RT correlations overall became less positive the closer to vocal-onset (*Wald* $\chi^2(1) = 13.79$, $p < 0.001$) and were maximal before 350 ms prior to vocal onset (Figure 4B). This was true for all or most patients depending on the brain structure (all patients in the lateral PFC, 4 of 5 in the lateral M1/PMC, 1 of 1 in the medial M1/PMC, but only one of two in the medial PFC; Figure S6B). There was also a main effect of Structure (*Wald* $\chi^2(3) = 10.44$, $p = 0.015$), HFB-RT correlations were overall more positive in the lateral M1/PMC than in the other frontal lobe structures.

In the stimulus-locked analysis of the frontal lobe, there were no significant effects of Window, Structure, or their interaction on HFB-RT correlations (Figure 4A, Figure S7A, and Table S7A).

In the temporal lobe, the HFB-RT correlation patterns were not as comparable to that of the Semantic Context effect both stimulus and response-locked (see SI).

Overall, where semantic interference was observed, stronger cortical response strength as indexed by HFB amplitude was associated with longer naming latencies. When word retrieval is more difficult, increased response-locked activity as a function of increasing reaction times is predominant in the frontal lobe (Figure 4B, and Figure S7B).

Frontal lobe vs. ITG interactions

We also investigated if cortical response strength co-varied between the main regions involved in word selection as indexed by the semantic interference effect (see SI for methods). Significant semantic

interference effects were found in the frontal lobe and in the ITG. Out of the six patients we tested with left hemisphere coverage, one had electrodes over both the frontal lobe (lateral and medial) and the ITG (i.e., ST32 whose electrodes are in dark blue in Figure S1). In this patient, we tested whether mean HFB correlated on a trial-by-trial basis between these sites.

In the stimulus-locked analysis, we found significant correlations between the lateral PFC and ITG between 400 and 1000 ms post-stimulus onset (rho= 0.437, $p_{corr} < .001$), corresponding to the interval where semantic interference was observed in these regions, but also between stimulus onset and 400 ms post-stimulus onset (rho= 0.313, $p_{corr} < .001$, see Figure S9A). This was not the case between the other frontal structures showing semantic interference effects and the ITG between 400 and 1000 ms post-stimulus onset, nor between stimulus onset and 400 ms post-stimulus onset (see SI).

Response-locked, we found significant correlations between the lateral PFC and ITG between -750 and -350 ms pre-vocal onset (rho= 0.518, $p_{corr} < .001$), corresponding to the interval where semantic interference was observed in these regions, but also between -350 ms and 250 ms around vocal-onset (rho= 0.505, $p_{corr} < .001$, see Figure S9B). This was also true between the medial PFC and the ITG between -750 and -350 ms post-stimulus onset (rho= 0.177, $p_{corr} = .027$) and between -350 ms and 250 ms around vocal-onset (rho= 0.204, $p_{corr} < .001$). Between the medial M1/PMC and the ITG, the correlation was only significant between -350 ms and 250 ms around vocal-onset (rho= 0.273, $p_{corr} < .001$) but not between -750 and -350 ms pre vocal-onset (see SI). This suggests that the lateral PFC and the medial PFC interact with the ITG on a trial-by-trial basis to support word retrieval. The later involvement of the medial M1/PMC suggests a possible role in verbal response monitoring, as suggested in (42) and (43).

Discussion

Our results present a detailed picture of the spatio-temporal cortical dynamics of lexical-semantic activation and word selection during overt speech production. Several conclusions can be drawn from our observations. First, semantic priming and interference effects were wide-spread across the cortical mantle and second, these effects co-existed in both time and in space. While the wide-spread distribution of the semantic system has been reported in several studies using fMRI (e.g.,44,45), word selection has usually been associated with a more restricted brain network, sometimes only highlighting one core brain region (i.e., the mid-section of the left MTG in [46], parts of the left MFG in [47]). Our results indicate that both lexical-semantic activation, as indexed by semantic priming, and word selection, as indexed by semantic interference, are supported by a wide network of left frontal and temporal brain regions. Second, in most time-windows we observed both semantic priming and interference co-occurring in different brain structures and in some structures, we observed both effects occurring sequentially. In particular, in the left ITG, semantic priming was observed until 400 ms and was then replaced by semantic interference. This, along with the absence of interaction between brain structure and semantic context, indicates that the division of labor between the two processes is not absolute. This is in disagreement with a simplified picture proposed in meta-analyses and reviews of language production (46,47), where brain regions are generally assigned one particular cognitive function, supporting a modular view of processing. Thus, in (47), the posterior ITG is associated with semantic processing but not with word retrieval which is supported by left PFC regions. Our results do not support this one-to-one mapping but instead suggest a given brain region may be involved in the spread of lexical-semantic activation as well as in subsequent word selection. These results help to reconcile computational models suggesting that the selection mechanism is external to the lexical-semantic activation system, in the sense of being hosted by brain regions external to the lexical-semantic system (e.g.,9), and models supporting a selection process internal to the lexical-semantic system (e.g., 7). In alignment with recent proposals (e.g., 48), our data support a widely distributed lexico-semantic model in which specific brain regions can be involved in more than one psycholinguistic process. We propose that such an organization is beneficial to optimal performance. Indeed, lexical-semantic activation and word selection are closely related and interdependent in speech production: one cannot in theory select a word without the prior activation of the lexicon (1,8). Thus, having the same cortical regions performing both processes could enhance word selection speed. An analogy with the motor and sensory cortices can be drawn with motor neurons found in the sensory cortex (49) and sensory neurons found in the motor cortex (50). Such an organization is believed to optimize sensory and motor adjustments respectively. A similar perspective can be used to understand our results shedding new light on our understanding of the neurobiological basis of language production.

A third key observation was that the temporal evolution of the semantic context effect depended on the brain structure engaged. In the left STG, MTG, ventral temporal cortex, but also in the lateral M1/PMC and medial PFC, semantic priming increased the further away from stimulus onset[5]. In other structures,

5

semantic interference increased the further away from stimulus onset and was maximal until 350 ms before vocal onset in all frontal structures. Therefore, during this sub-second time scale of observation, semantic priming was predominant in some structures while semantic interference was predominant in others. The brain structures we found to predominantly reflect semantic priming have previously been associated with lexical-semantic activation in both language production and comprehension, especially for the temporal lobe structures (19,20,23,51,52). The semantic priming effects found in the lateral M1/PMC could be attributed to possible interactions between this area and semantic processing though the causal role of this region in the representation of semantic knowledge is unclear (53). Conversely, brain regions found to mostly reflect semantic interference have been previously associated with word selection, especially the lateral PFC and medial frontal cortex (12,18,23,54). The posterior ITG has been associated with semantics (47), but also with lexical access as evidenced by negative correlations between anomic rate and resting state brain metabolism in this area (21). Our results reconcile these interpretations and suggest this brain region may be involved in both processes at different time-points. The semantic priming and interference effects reached their maxima around the same time (on average between 600 and 800 ms after stimulus onset). Thus, our results support temporal overlap between lexical-semantic activation and word selection, suggesting lexical-semantic activation does not end when word selection starts. This is in agreement with most language production models, in which some degree of cascaded processing between lexical-semantic activation and word selection is allowed (e.g. 1,8,41). In addition, the fact the semantic interference effect was mainly present before 350 ms prior to vocal onset is in agreement with the chronometric estimates provided by (46). This suggests the word selection process is mostly over by this point in time, leaving time for the subsequent phonological encoding and articulatory processes to take place.

A similar division between temporal and frontal regions was observed in the HFB-RT correlation patterns. Frontal regions which showed an overall larger semantic interference effect showed stronger cortical response strength associated with longer reaction times, especially time-locked to vocal-onset. This is similar to observations in other cognitive domains such as in working memory tasks, where gamma-band (30-60 Hz) amplitude in the frontal cortex increases with memory load (55). Mirroring the semantic interference effect, HFB-RT correlation coefficients were maximal up to 350 ms before vocal onset. These results are in agreement with the idea that the frontal cortex engages as a function of trial-by-trial difficulty in language production as in other cognitive functions. In the context of this picture-naming task, the frontal cortex seems to play an adaptive cognitive control role in interference resolution for word selection.

Finally, HFB power was correlated trial-by-trial between the lateral PFC and medial PFC and the ITG in

---

There was a reversal of polarity from semantic interference to semantic priming in 4 out of 5 patients in the lateral M1/PMC (Figure S6, such consistency was not observed for the other structures showing an increase in semantic priming with time). The initial interference effect may be reflecting an early preparation signal from this structure to the other regions subsequently involved in word selection, although further research is needed to determine the functional significance of this effect.

the time-windows where semantic interference effects were observed supporting the idea that the left PFC interacts with the left ITG in a trial-by-trial manner to support word selection. One caveat concerning the spatial and temporal precision of our claims is worth mentioning. ECoG recording restrictions resulted in sparse and spatially-biased spatial sampling, this constraint required collapsing across broad cortical structures for statistical analysis (as in 56). Here, we also collapsed our analysis over 200-ms time-windows in order to simultaneously test for spatial and temporal effects, thus limiting our temporal resolution to this scale.

To conclude, these results provide new insights into the cortical dynamics of word retrieval in speech production. Our results show that a widespread network of brain regions supports different aspects of word retrieval. Both medial and left PFC regions are involved in trial-by-trial interactions with the posterior ITG to help overcome interference caused by semantically-related alternatives in word selection. Finally, unlike prior concepts of a strict modular organization of word retrieval, our ECoG results show that the same brain region may be involved in both lexical-semantic activation as well as word selection in different time-windows.

Methods

1. Participants

Nine patients (3 women, median age at time of testing: 26 years old, IQR = 23-42 years old), undergoing neurological treatment for refractory epilepsy participated in the study. During clinical treatment, the patients were implanted with 74-157 electrodes (grids and strips, electrode spacing: 0.6-1 cm), covering extensive portions of the lateral cortices in both hemispheres (Figure S1). Seven patients had left and two patients had right hemisphere coverage. Electrode placement and medical treatment were dictated solely by the clinical needs of the patient. Electrophysiological signals were monitored by clinicians for approximately one week. During lulls in clinical treatment, patients willing to participate in the study provided written and oral informed consent. Patients were tested at six different institutions: Stanford Hospital, Stanford, CA; California Pacific Medical Center, San Francisco, CA; UCSF Benioff Children's Hospital and Research Center, Oakland, CA; UC Irvine Health, Irvine, CA; Albany Medical College, Albany, NY; The Johns Hopkins Hospital, Baltimore, MD. The institutional review board of each institution approved the research that was conducted at each respective location. Anti-epileptic medications were discontinued 2-3 days beforehand, and patients were seizure free for at least five hours before testing. All individuals had normal language, normal or corrected-to-normal vision, and were native speakers of English (n=8) or Spanish (n=1). They all performed the task using their native language. All but one patient were right-handed and the one left-handed patient was left-hemisphere dominant for language.

2. Material and Design

The stimuli were 550 x 240 pixels high line drawings of common objects or animals selected from published collections (57,58). Their name agreement was very high (median = 95%; IQR = 90-99%). They were presented in free viewing on a laptop computer screen 50-60 cm from the patient's eyes. A total of 16 pictures were used in the experiment. They were issued from 4 different semantic categories (clothing items, animals, musical instruments, and human dwellings), and were presented 4 times within HOM versus HET blocks (11). Because participants also performed a Simon task (59) (not reported here), the pictures were colored in green or purple and were presented on the left or the right of the fixation point. Within each experimental run, the order in which the items were presented was mixed pseudorandomly using the software MIX (60) such that consecutive items were phonologically unrelated, i.e., two pictures in a row never had the same initial phoneme.

3. Procedure

The experiment was controlled by Eprime 2.0 Professional (Psychology Software Tools, Inc., Pittsburgh, PA) or BCI2000 (61) (2 patients), allowing online recording of the participants' verbal response. A trial consisted of the following events: (1) a fixation point ("plus" sign presented at the center of the screen) for 500 ms; (2) a picture for 2000 ms which participants had to name as fast and as accurately as possible (3) a blank screen for 2000 ms. Underneath a photodiode placed at the bottom left of the screen, a white

rectangle appeared and disappeared along with the stimulus to mark the onset and offset of picture presentation. Vocal-onsets were used as the response-onset measure. There were 4 blocks of 32 trials each. The participant could rest for as long as necessary between blocks. Before the task, participants were familiarized with the picture names and the experimenter made verbal corrections when an incorrect response was produced. The experimental session lasted 10 to 15 minutes.

4. Data acquisition

Verbal responses were acquired at a sampling rate of 44 kHz. Electrophysiological and peripheral data (photodiode and microphone input) were acquired simultaneously using a 128-channel Tucker Davis Technologies recording system at Stanford (3052 Hz digitization), a 128-channel Nihon Kohden recording system (Nihon Kohden Corporation) at CPMC, Children's Hospital, and UC Irvine (1000 Hz digitization), a 112-channel g.USBamp biosignal acquisition system (g.tec, Graz, Austria, 9600Hz digitization) at Albany Medical College, and a 128-channel Stellate Harmonie recording system (Natus Medical, Inc.; 1000 Hz digitization) at Johns Hopkins. Data were recorded using a subdural electrode reference and a scalp ground.

5. Electrode localization

Structural preoperative magnetic resonance imaging (MRI) and post-implantation computerized tomography (CT) scans were acquired for each patient. These scans were coregistered to the same space using two nonlinear transformations based on normalized mutual information implemented in the Bioimage suite (62), as in (25). The second transformation was used to correct for slight shifts in brain morphology caused by the electrodes. The results were then compared with an intraoperative photo image of the exposed grid after it was sutured to the dura. Brains and electrodes were transformed into MNI space across subjects only for visual display. Electrodes were classified according to their anatomical location within each patient's anatomical space. Electrode location was coded according to 2 levels: lobe (frontal and temporal), and structure (regrouping one or several gyri). The frontal lobe was divided into 4 structures: the lateral and medial primary motor and premotor cortex (M1/PMC) grouping frontal electrodes on or posterior to the precentral sulcus and anterior to the Rolandic sulcus, the lateral and medial prefrontal cortex grouping the inferior, middle, and superior frontal gyrus (IFG, MFG, and SFG, respectively). The orbito-frontal and fronto-polar cortices (grouping the ventral part of the frontal lobe and the most anterior part of the SFG and MFG, as defined by being anterior to the IFG's anterior boundary but lying ventral to the anterior commissure axis) were not included in the analysis. The temporal lobe was divided into 4 structures: the superior temporal gyrus (STG), the middle and inferior temporal gyri (MTG and ITG), and the ventral temporal lobe (not including the electrodes also visible on the lateral views). Each patient's electrode location was defined by a neurologist.

6. Data pre-processing and analysis

6.1. Behavioral data

The accuracy of the responses and the verbal reaction times were measured offline using CheckVocal (63). Trials were excluded from the analysis of the correct responses if the participant did not respond, or produced any kind of verbal error: partial or complete production of incorrect words, verbal dysfluencies (stuttering, utterance repairs, etc.).

Statistical analysis was performed within R version 3.1.1 (64) using the packages "lme4" to compute the mixed effect models (50) and "car" to compute analysis of deviance tables for the fixed effects of the mixed effect models (65). We analyzed the data using generalized linear (for reaction times) and logistic (for accuracy rates) mixed-effects models (66,67). The analyses were performed on log-transformed RTs and accuracy rates. We tested for fixed effects of Semantic Context (HOM vs. HET), Presentation Number (from 2 to 4), and Stimulus Position (i.e., left or right of the fixation cross) as within-subject factors, and the interaction between Semantic Context and Presentation Number. As random effects, we had intercepts for participants and picture name, as well as by-subject random slopes for within-subject factors. P-values were obtained using type-III (because of the presence of an interaction) analyses-of-deviance tables providing Wald chi-square tests for the fixed effects in the generalized linear mixed-effects models. For all models, we report Wald χ^2-values and p-values from the analysis of deviance tables (in the main text), as well as raw β estimates (β_{raw}), 95% confidence intervals around these β estimates (CI), standard errors, t-values for reaction times, and Wald Z and associated p-values for significant effects on accuracy rates (in the SI).

6.2. ECoG data

All ECoG channels were inspected by a neurologist to identify those with epileptiform activity and artifacts (e.g., due to poor contact or high frequency noise). These channels and those that were located over tissue that was later resected were removed from the analysis. Epochs containing local artifacts on otherwise normal channels were removed from the analysis as well. Raw, continuous data were down-sampled to 1,000 Hz, and filtered with a 60 Hz notch filter as described in (68). The ECoG data were then re-referenced to a common average reference (defined as the mean of the remaining channels). Single channels of this ECoG data are referred to as "raw signal".

The analytic amplitude (or power) of HFB was extracted from the raw signal using a frequency-domain half-max, full-width Gaussian filter along with a Hilbert transform (as in 25). The time-course of the HFB power was then smoothed using a Hanning window (50 samples), segmented time-locked to stimulus (between -1000 and 2000 ms around stimulus onset) and vocal-onset (between -1500 and 500 ms around vocal onset), and normalized to baseline power (stimulus-locked baseline: -1000 to -500 ms pre-stimulus onset; response-locked baseline: -1500 to -1000 ms pre-vocal onset; resulting unit of HFB power in percent change from baseline) for all correct artifact-free trials. We tested whether an electrode had significant HFB or not by comparing the HFB power in each trial to zero using one-sided Student t-tests assuming unequal variance on consecutive 50-ms-long time-windows between 0 and 1000 ms time-locked to the

stimulus and between -750 and 250 ms around vocal-onset. The rate of type I errors in null hypothesis testing was controlled for by calculating the false discovery rate (FDR) on the resulting p-values. An electrode was considered "active" if it had at least one 50-ms-long segment which had significant HFB power after FDR correction (Figure S3).

To test for the time-course of experimental effects, we averaged the HFB power in each trial over one to five 200-ms-long consecutive time-windows for each active electrode stimulus and response-locked (Figures 2, 3, and 4). The number of time-windows included in the analysis for each electrode was determined by whether or not this electrode had significant HFB in the specific time-window as determined by the prior HFB significance testing. We used the same time-windows in each trial for a given electrode. We then ran mixed-effect models on within-trial mean HFB as the dependent variable controlling for the time-Window (1 to 5), Structure, as well as the same parameters as for the behavioral data. We ran separate models for each cerebral lobe of interest (i.e., frontal and temporal) and tested for fixed effects of Semantic Context (HOM vs. HET), Presentation Number (from 2 to 4; the first presentation was removed from the analysis of the ECoG data similarly as for the behavioral data), Window (1 to 5), Structure, and Stimulus Position (i.e., left or right of the fixation cross) as within-subject factors, and the interactions between Semantic Context and Presentation Number, as well as between Semantic Context, Window, and Structure. As random effects, we had intercepts for picture name, and participant, as well as by-participant random slopes for the fixed effects of interest (i.e., Semantic Context, Window, their interaction, and Presentation Number[6]). We could not control for Structure in the random slopes given not every participant had electrodes in each Structure, but show in Figure S6 that the fixed effects involving Structure were present in a majority of patients. P-values were obtained similarly as for the behavioral analyses. For illustrative purposes (Figure 2), the same models were also run per electrode stimulus and response-locked.

6 We could not include a random slope for the interaction between Presentation Number and Semantic Context as the models would not converge with this level of complexity. However, no interaction between Semantic Context and Presentation Number were found in the fixed effects for any of the models.

Acknowledgements

This research was supported by a post-doctoral grant from the National Institute on Deafness and Other Communication Disorders of the National Institutes of Health under Award Number F32DC013245 to S.K.R., NIH grants EB00856, EB006356 and EB018783, the US Army Research Office grants W911NF-08-1-0216, W911NF-12-1-0109, W911NF-14-1-0440 and Fondazione Neurone to G.S., NINDS grant R01NS078396 and NSF grant BCS1358907 to J.P., NINDS grant NS40596 to N.E.C, grants 10F-RCS-006 and CX000254 from the US Department of Veterans Affairs Clinical Sciences Research and Development Program to N.F.D., and NINDS grant 2R37NS21135 and the Nielsen Corporation to R.T.K.. The content is solely the responsibility of the authors and does not necessarily represent the official views of the National Institutes of Health, the Department of Veterans Affairs, or the United States government. We would like to thank Matar Haller, Augusta Shestyuk, and Adeen Flinker for technical input, James Lubell and Callum Dewar for creating subject reconstructions, and all members of the Knight laboratory for their help with data recording. Finally, we are very thankful to the research volunteers who took part in this study.

References

1. Levelt WJ, Roelofs A, Meyer AS. A theory of lexical access in speech production. Behav Brain Sci. 1999 Feb;22(1):1-38-75.

2. Understanding Aphasia, 1st Edition | Harold Goodglass | ISBN 9780122900402 [Internet]. [cited 2016 Sep 10]. Available from: http://store.elsevier.com/Understanding-Aphasia/Harold-Goodglass/isbn-9780122900402/

3. Kutas null, Federmeier null. Electrophysiology reveals semantic memory use in language comprehension. Trends Cogn Sci. 2000 Dec 1;4(12):463–70.

4. Navarrete E, Del Prato P, Mahon BZ. Factors determining semantic facilitation and interference in the cyclic naming paradigm. Front Psychol. 2012;3:38.

5. Navarrete E, Del Prato P, Peressotti F, Mahon BZ. Lexical Retrieval is not by Competition: Evidence from the Blocked Naming Paradigm. J Mem Lang. 2014 Oct;76:253–72.

6. Roelofs A, Piai V. Aspects of competition in word production: reply to Mahon and Navarrete. Cortex J Devoted Study Nerv Syst Behav. 2015 Mar;64:420–4.

7. Howard D, Nickels L, Coltheart M, Cole-Virtue J. Cumulative semantic inhibition in picture naming: experimental and computational studies. Cognition. 2006 Jul;100(3):464–82.

8. Dell GS. A spreading-activation theory of retrieval in sentence production. Psychol Rev. 1986 Jul;93(3):283–321.

9. Oppenheim GM, Dell GS, Schwartz MF. The dark side of incremental learning: a model of cumulative semantic interference during lexical access in speech production. Cognition. 2010 Feb;114(2):227–52.

10. qkj8202.PDF - Kroll & Stewart.pdf [Internet]. [cited 2016 Nov 23]. Available from: http://www.pitt.edu/~perfetti/PDF/Kroll%20&%20Stewart.pdf

11. Damian MF, Vigliocco G, Levelt WJ. Effects of semantic context in the naming of pictures and words. Cognition. 2001 Oct;81(3):B77-86.

12. Schnur TT, Schwartz MF, Kimberg DY, Hirshorn E, Coslett HB, Thompson-Schill SL. Localizing interference during naming: convergent neuroimaging and neuropsychological evidence for the function of Broca's area. Proc Natl Acad Sci U S A. 2009 Jan 6;106(1):322–7.

13. Ries SK, Greenhouse I, Dronkers NF, Haaland KY, Knight RT. Double dissociation of the roles of the left and right prefrontal cortices in anticipatory regulation of action. Neuropsychologia. 2014 Oct;63:215–25.

14. Maess B, Friederici AD, Damian M, Meyer AS, Levelt WJM. Semantic category interference in overt picture naming: sharpening current density localization by PCA. J Cogn Neurosci. 2002 Apr 1;14(3):455–62.

15. Janssen N, Hernández-Cabrera JA, van der Meij M, Barber HA. Tracking the Time Course of Competition During Word Production: Evidence for a Post-Retrieval Mechanism of Conflict Resolution. Cereb Cortex N Y N 1991. 2015 Sep;25(9):2960–9.

16. Aristei S, Melinger A, Abdel Rahman R. Electrophysiological chronometry of semantic context effects in language production. J Cogn Neurosci. 2011 Jul;23(7):1567–86.

17. Tremblay P, Gracco VL. Contribution of the pre-SMA to the production of words and non-speech oral motor gestures, as revealed by repetitive transcranial magnetic stimulation (rTMS). Brain Res. 2009 May 1;1268:112–24.

18. Alario F-X, Chainay H, Lehericy S, Cohen L. The role of the supplementary motor area (SMA) in word production. Brain Res. 2006 Mar 3;1076(1):129–43.

19. Piai V, Roelofs A, Acheson DJ, Takashima A. Attention for speaking: domain-general control from the anterior cingulate cortex in spoken word production. Front Hum Neurosci. 2013;7:832.

20. Baldo JV, Arévalo A, Patterson JP, Dronkers NF. Grey and white matter correlates of picture naming: evidence from a voxel-based lesion analysis of the Boston Naming Test. Cortex J Devoted Study Nerv Syst Behav. 2013 Mar;49(3):658–67.

21. Trebuchon-Da Fonseca A, Guedj E, Alario F-X, Laguitton V, Mundler O, Chauvel P, et al. Brain regions underlying word finding difficulties in temporal lobe epilepsy. Brain J Neurol. 2009 Oct;132(Pt 10):2772–84.

22. de Zubicaray GI, Hansen S, McMahon KL. Differential processing of thematic and categorical conceptual relations in spoken word production. J Exp Psychol Gen. 2013 Feb;142(1):131–42.

23. Piai V, Roelofs A, Jensen O, Schoffelen J-M, Bonnefond M. Distinct patterns of brain activity characterise lexical activation and competition in spoken word production. PloS One. 2014;9(2):e88674.

24. Edwards E, Nagarajan SS, Dalal SS, Canolty RT, Kirsch HE, Barbaro NM, et al. Spatiotemporal imaging of cortical activation during verb generation and picture naming. NeuroImage. 2010 Mar;50(1):291–301.

25. Flinker A, Korzeniewska A, Shestyuk AY, Franaszczuk PJ, Dronkers NF, Knight RT, et al. Redefining the role of Broca's area in speech. Proc Natl Acad Sci U S A. 2015 Mar 3;112(9):2871–5.

26. Bouchard KE, Mesgarani N, Johnson K, Chang EF. Functional organization of human sensorimotor cortex for speech articulation. Nature. 2013 Mar 21;495(7441):327–32.

27. Hamamé CM, Alario F-X, Llorens A, Liégeois-Chauvel C, Trébuchon-Da Fonseca A. High frequency gamma activity in the left hippocampus predicts visual object naming performance. Brain Lang. 2014 Aug;135:104–14.

28. Llorens A, Dubarry A-S, Trébuchon A, Chauvel P, Alario F-X, Liégeois-Chauvel C. Contextual modulation of hippocampal activity during picture naming. Brain Lang. 2016 Aug;159:92–101.

29. Piai V, Anderson KL, Lin JJ, Dewar C, Parvizi J, Dronkers NF, et al. Direct brain recordings reveal hippocampal rhythm underpinnings of language processing. Proc Natl Acad Sci U S A. 2016 Oct 4;113(40):11366–71.

30. Abdel Rahman R, Melinger A. When bees hamper the production of honey: lexical interference from associates in speech production. J Exp Psychol Learn Mem Cogn. 2007 May;33(3):604–14.

31. Belke E, Meyer AS, Damian MF. Refractory effects in picture naming as assessed in a semantic blocking paradigm. Q J Exp Psychol A. 2005 May;58(4):667–92.

32. Ewald A, Aristei S, Nolte G, Abdel Rahman R. Brain Oscillations and Functional Connectivity during Overt Language Production. Front Psychol. 2012;3:166.

33. Llorens A, Trébuchon A, Liégeois-Chauvel C, Alario F-X. Intra-cranial recordings of brain activity during language production. Front Psychol. 2011;2:375.

34. Flinker A, Chang EF, Kirsch HE, Barbaro NM, Crone NE, Knight RT. Single-trial speech suppression of auditory cortex activity in humans. J Neurosci Off J Soc Neurosci. 2010 Dec 8;30(49):16643–50.

35. Ray S, Maunsell JHR. Different origins of gamma rhythm and high-gamma activity in macaque visual cortex. PLoS Biol. 2011 Apr;9(4):e1000610.

36. Halgren E, Baudena P, Heit G, Clarke JM, Marinkovic K, Clarke M. Spatio-temporal stages in face and word processing. I. Depth-recorded potentials in the human occipital, temporal and parietal lobes [corrected]. J Physiol Paris. 1994;88(1):1–50.

37. Halgren E, Baudena P, Heit G, Clarke JM, Marinkovic K, Chauvel P, et al. Spatio-temporal stages in face and word processing. 2. Depth-recorded potentials in the human frontal and Rolandic cortices. J Physiol Paris. 1994;88(1):51–80.

38. Marinković K. Spatiotemporal dynamics of word processing in the human cortex. Neurosci Rev J Bringing Neurobiol Neurol Psychiatry. 2004 Apr;10(2):142–52.

39. Kam J, Szczepanski S, Canolty RT, Flinker A, Auguste K, Crone NE, et al. Differential Sources for Two Neural Signatures of Target Detection: An Electrocorticography Study. in press;

40. Szczepanski SM, Crone NE, Kuperman RA, Auguste KI, Parvizi J, Knight RT. Dynamic changes in phase-amplitude coupling facilitate spatial attention control in fronto-parietal cortex. PLoS Biol. 2014 Aug;12(8):e1001936.

41. Roelofs A. A spreading-activation theory of lemma retrieval in speaking. Cognition. 1992 Mar;42(1–3):107–42.

42. Riès S, Janssen N, Dufau S, Alario F-X, Burle B. General-purpose monitoring during speech production. J Cogn Neurosci. 2011 Jun;23(6):1419–36.

43. Nozari N, Dell GS, Schwartz MF. Is comprehension necessary for error detection? A conflict-based account of monitoring in speech production. Cognit Psychol. 2011 Aug;63(1):1–33.

44. Binder JR, Desai RH, Graves WW, Conant LL. Where is the semantic system? A critical review and meta-analysis of 120 functional neuroimaging studies. Cereb Cortex N Y N 1991. 2009 Dec;19(12):2767–96.

45. Huth AG, de Heer WA, Griffiths TL, Theunissen FE, Gallant JL. Natural speech reveals the semantic maps that tile human cerebral cortex. Nature. 2016 Apr 28;532(7600):453–8.

46. Indefrey P. The spatial and temporal signatures of word production components: a critical update. Front Psychol. 2011;2:255.

47. Price CJ. A review and synthesis of the first 20 years of PET and fMRI studies of heard speech, spoken language and reading. NeuroImage. 2012 Aug 15;62(2):816–47.

48. Strijkers K, Costa A. The cortical dynamics of speaking: present shortcomings and future avenues. Lang Cogn Neurosci. 2016 Apr 20;31(4):484–503.

49. Matyas F, Sreenivasan V, Marbach F, Wacongne C, Barsy B, Mateo C, et al. Motor control by sensory cortex. Science. 2010 Nov 26;330(6008):1240–3.

50. Evarts EV, Fromm C. Sensory responses in motor cortex neurons during precise motor control. Neurosci Lett. 1977 Aug;5(5):267–72.

51. Clarke A, Taylor KI, Devereux B, Randall B, Tyler LK. From perception to conception: how meaningful objects are processed over time. Cereb Cortex N Y N 1991. 2013 Jan;23(1):187–97.

52. Dronkers NF, Wilkins DP, Van Valin RD, Redfern BB, Jaeger JJ. Lesion analysis of the brain areas involved in language comprehension. Cognition. 2004 Jun;92(1–2):145–77.

53. Andres M, Olivier E, Badets A. Actions, Words, and Numbers A Motor Contribution to Semantic Processing? Curr Dir Psychol Sci. 2008 Oct 1;17(5):313–7.

54. Thompson-Schill SL, D'Esposito M, Aguirre GK, Farah MJ. Role of left inferior prefrontal cortex in retrieval of semantic knowledge: a reevaluation. Proc Natl Acad Sci U S A. 1997 Dec 23;94(26):14792–7.

55. Howard MW, Rizzuto DS, Caplan JB, Madsen JR, Lisman J, Aschenbrenner-Scheibe R, et al. Gamma oscillations correlate with working memory load in humans. Cereb Cortex N Y N 1991. 2003 Dec;13(12):1369–74.

56. Voytek B, Kayser AS, Badre D, Fegen D, Chang EF, Crone NE, et al. Oscillatory dynamics coordinating human frontal networks in support of goal maintenance. Nat Neurosci. 2015 Sep;18(9):1318–24.

57. Snodgrass JG, Vanderwart M. A standardized set of 260 pictures: Norms for name agreement, image agreement, familiarity, and visual complexity. J Exp Psychol [Hum Learn]. 1980 Mar;6(2):174.

58. Bonin P, Peereman R, Malardier N, Méot A, Chalard M. A new set of 299 pictures for psycholinguistic studies: French norms for name agreement, image agreement, conceptual familiarity, visual complexity, image variability, age of acquisition, and naming latencies. Behav Res Methods Instrum Comput. 2003 Feb 1;35(1):158–67.

59. Craft JL, Simon JR. Processing symbolic information from a visual display: interference from an irrelevant directional cue. J Exp Psychol. 1970 Mar;83(3):415–20.

60. van Casteren M, Davis MH. Mix, a program for pseudorandomization. Behav Res Methods. 2006 Nov;38(4):584–9.

61. Schalk G, McFarland DJ, Hinterberger T, Birbaumer N, Wolpaw JR. BCI2000: a general-purpose brain-computer interface (BCI) system. IEEE Trans Biomed Eng. 2004 Jun;51(6):1034–43.

62. Papademetris X, Jackowski MP, Rajeevan N, DiStasio M, Okuda H, Constable RT, et al. BioImage Suite: An integrated medical image analysis suite: An update. Insight J. 2006;2006:209.

63. Protopapas A. CheckVocal: a program to facilitate checking the accuracy and response time of vocal responses from DMDX. Behav Res Methods. 2007 Nov;39(4):859–62.

64. R Core Team. R: A language and environment for statistical computing. R Found Stat Comput Vienna Austria [Internet]. 2014; Available from: http://www.R-project.org/

65. Fox J, Weisberg S. An R Companion to Applied Regression. Sage Publishing. 2011.

66. Baayen RH, Davidson DJ, Bates DM. Mixed-effects modeling with crossed random effects for subjects and items. J Mem Lang. 2008 Nov;59(4):390–412.

67. Jaeger TF. Categorical Data Analysis: Away from ANOVAs (transformation or not) and towards Logit Mixed Models. J Mem Lang. 2008 Nov;59(4):434–46.

68. Keren AS, Yuval-Greenberg S, Deouell LY. Saccadic spike potentials in gamma-band EEG: characterization, detection and suppression. NeuroImage. 2010 Feb 1;49(3):2248–63.

Figures:

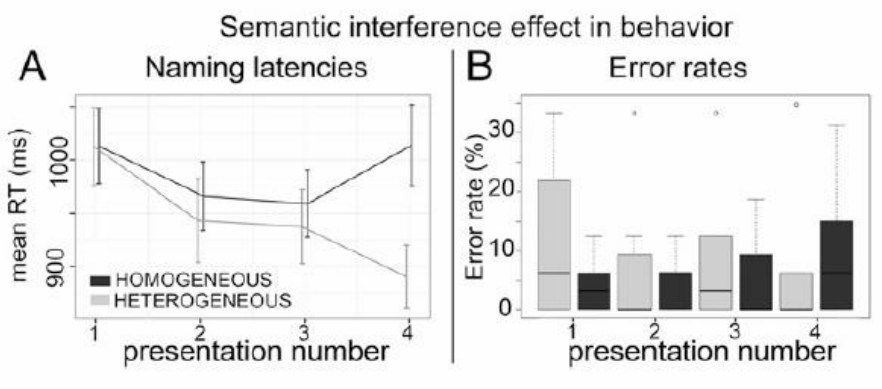

Figure 1: Semantic interference effect on mean reaction times (A) and median error rates (B). Values for homogeneous blocks (HOM) are in dark gray and values for heterogeneous blocks (HET) are in light gray. Values for presentation numbers 1 to 4 are presented although only presentation numbers 2 to 4 were included in the analyses. For reaction times (A), standard deviations are represented by the horizontal lines. For error rates (B), medians are indicated by the black horizontal lines in the box-and-whisker plots. Interquartile ranges are represented by the boxes and the total range is depicted by the dotted lines.

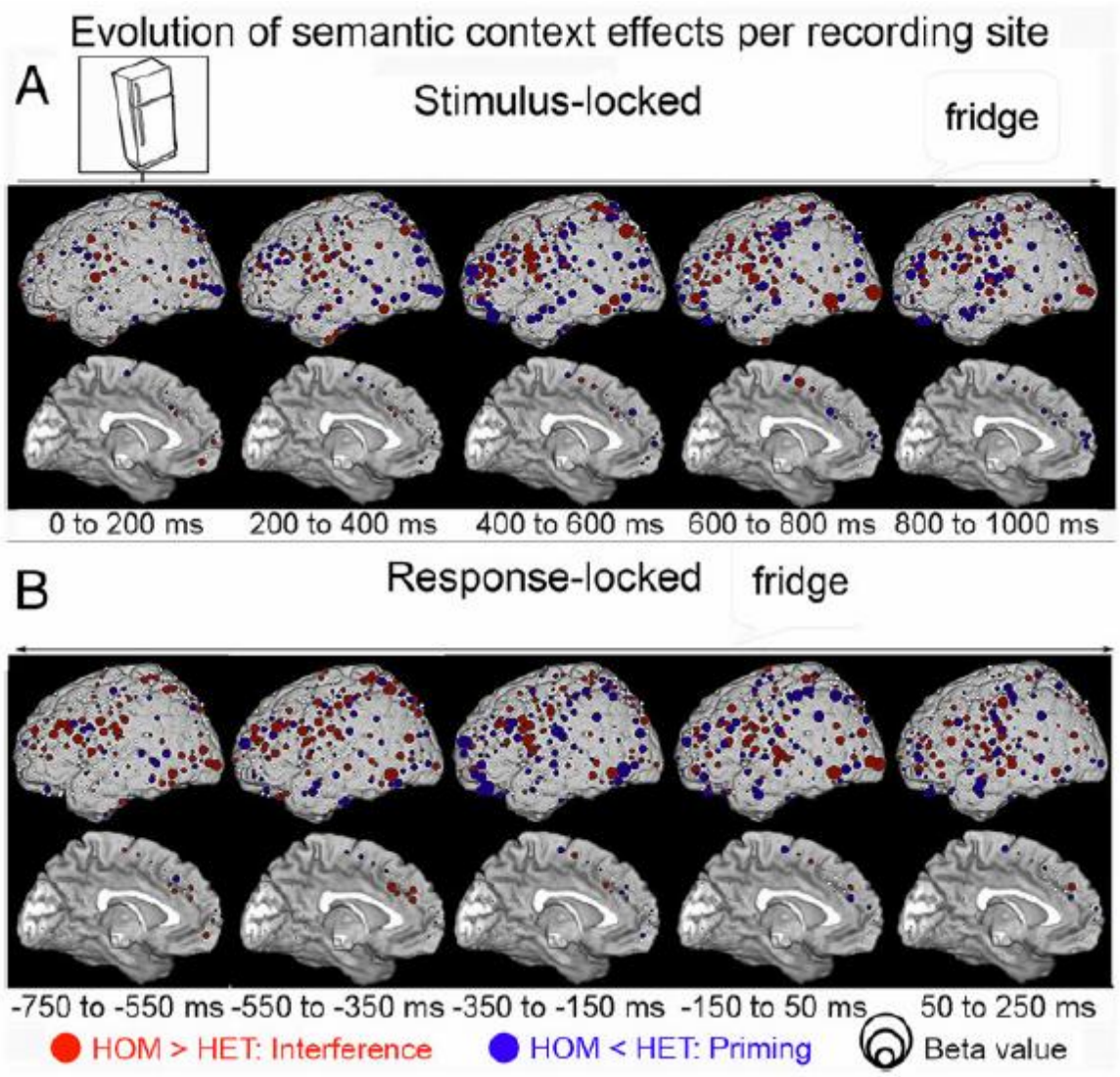

Figure 2: Evolution of the semantic context effect per recording site stimulus (A) and response-locked (B) on the left lateral and medial views of the MNI brain. Each column corresponds to one of 5 time-windows of analyses. Electrodes colored in red correspond to electrodes showing more HFB activity in HOM than HET blocks (in the direction of the semantic interference effect), electrodes colored in blue correspond to electrodes showing more HFB in HET than HOM blocks (in the direction of semantic priming), as estimated with the linear mixed effect models ran for each electrode for visual purposes. The size of the dots is proportional to the raw β values for the main effect of semantic context.

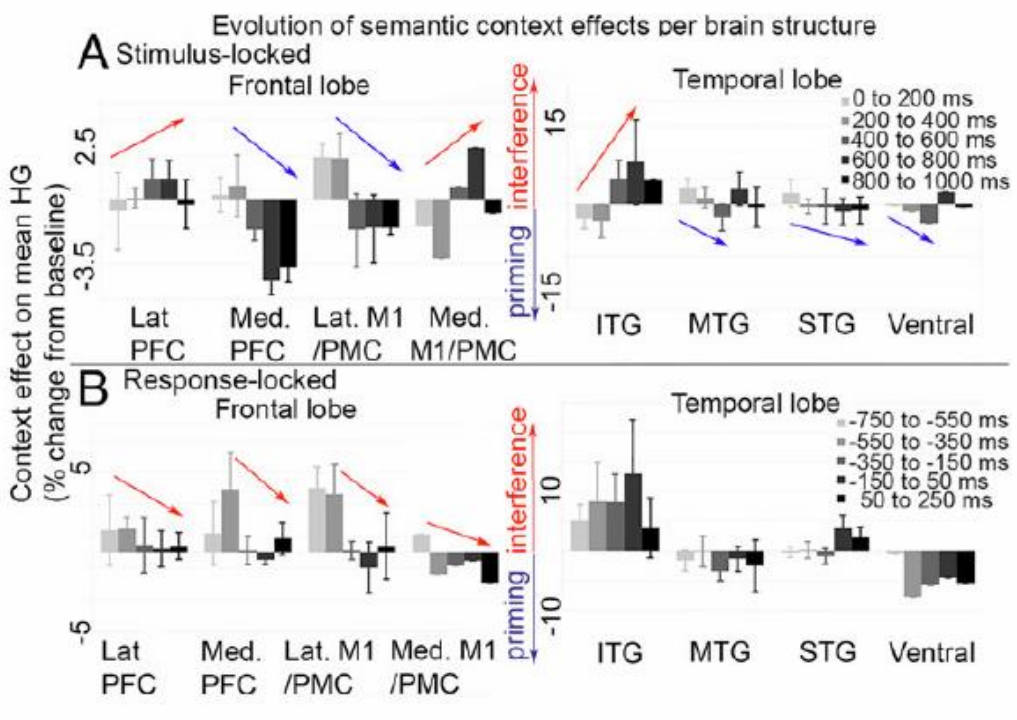

Figure 3: Evolution of the size of the semantic context effect on the mean HFB per brain structure in the frontal and temporal lobe stimulus (A) and response-locked (B). Time-windows are color-coded in 5 shades of gray (from light to dark). Positive values correspond to semantic interference effects (more HFB activity in HOM than HET blocks), negative values correspond to semantic priming effects (more HFB in HET than HOM blocks). Red and blue arrows indicate the direction of the Semantic Context by Window interactions in each brain structure. Ventral views are presented in Figure S5.

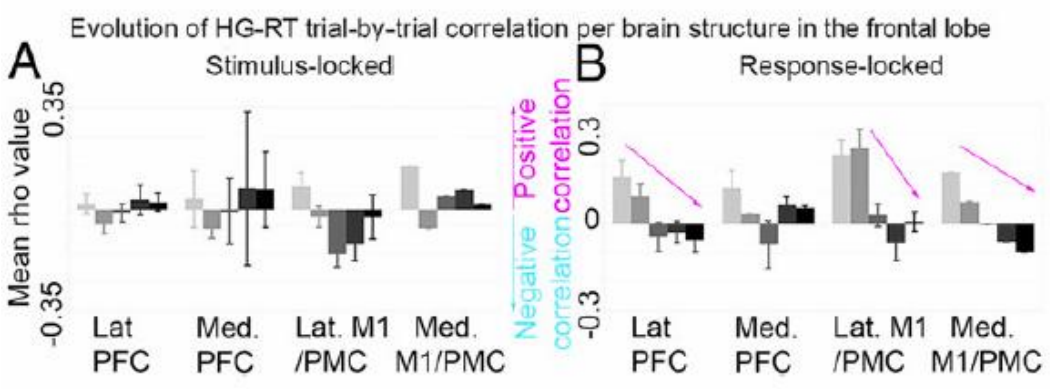

Figure 4: Evolution of the HFB-RT correlation coefficient per brain structure in the frontal lobe stimulus (A) and response-locked (B). Time-windows are color-coded in 5 shades of gray (from light to dark). Positive values correspond to positive HFB-RT correlations (more HFB associated with longer RTs), negative values correspond to negative HFB-RT correlations (more HFB associated with shorter RTs). Pink and aqua arrows indicate the direction of the HFB-RT correlation by Window interactions in each brain structure.

Supplementary Information Appendix

Supplementary figures are included at the end of the appendix.

1. **Methods – correlation tests**

We examined how mean HFB per time-window was correlated with reaction times (as measured with naming latencies) using non-parametric Spearman rank correlation tests. We calculated the associated rho correlation coefficient per time-window and per electrode and analyzed the evolution of these coefficients over time stimulus and response-locked in the frontal and temporal lobes using similar mixed effect models as for the experimental manipulations. We tested for fixed effects of Structure and Window and their interaction. The variability between patients was controlled for using Patient as a random effect, as well as a by-patient random slope for Window. We could not control for Structure in the random slope given not every participant had electrodes in each Structure, but show in Figure S6 that the fixed effects involving Structure were present in a majority of patients.

We tested for whether or not the mean HFB power per trial between structures showing a significant semantic interference effect was correlated between structures using the non-parametric Spearman's rank correlation coefficient. Associated p-values were bonferroni-corrected for the number of tests performed. This analysis aimed to inform the possible interactions occurring between distributed cortical sites responsive to the semantic interference effect (Figure S8).

2. **Behavioral results**

Participant had a marginal repetition priming effect on log-transformed naming latencies (*Wald* $\chi^2(1) = 2.84$, $p = .092$; Table S2 A). There was no effect of Stimulus Position (*Wald* $\chi^2(1) = 1.36$, $p = .244$; pictures were presented on the left or on the right of the fixation cross for purposes unrelated to the present study).

There was no significant effect of any of the experimental parameters we controlled for on accuracy rates: Semantic context: *Wald* $\chi^2(1) = 0.69$, $p = .406$; Presentation number: *Wald* $\chi^2(1) = 0.54$, $p = .464$; Stimulus Position: *Wald* $\chi^2(1) = 0.03$, $p = .872$; Semantic Context by Presentation number: *Wald* $\chi^2(1) = 1.59$, $p = .207$ (Table S2 B).

Table S1: Mean naming latencies (A) and median error rates (B) and per presentation number within category. Standard deviations (for reaction times) and interquartile ranges (for error rates) are in brackets.

A. Naming latencies (in msec)

	Presentation number (#)				
	1	2	3	4	Average
HOM	1013 (200)	966 (182)	959 (178)	1014 (215)	988 (185)
HET	1013 (209)	943 (223)	937 (195)	890 (168)	945 (195)

B. Error rates (in %)

	Presentation number (#)				
	1	2	3	4	Average
HOM	3 (0-6)	6 (0-6)	0 (0-5)	6 (0-14)	5 (2-10)
HET	6 (0-20)	0 (0-8)	3 (0-13)	0 (0-6)	5 (1-9)

Table S2: Fixed effects output of the mixed effect models on naming latencies (A) and accuracy rates (B): Beta coefficients (raw, in log-scale), confidence intervals for the beta coefficients (CI: lower and upper bound in log-scale), standard errors (SE), t (for naming latencies) and Z (for accuracy rates) -values for each of the fixed effects in the mixed effect models Effects reported in the main manuscript are in bold.

A. Fixed effects of the mixed effect model on log-transformed naming latencies					
	β raw	*CI (lower)*	*CI (upper)*	*SE*	*t-Value*
Intercept	6.77	6.62	6.93	8.00×10^{-2}	84.62
Semantic Context	$\mathbf{5.66 \times 10^{-2}}$	$\mathbf{0.61 \times 10^{-2}}$	$\mathbf{10.71 \times 10^{-2}}$	$\mathbf{2.58 \times 10^{-2}}$	**2.20**
Presentation Number	-2.40×10^{-2}	-5.20×10^{-2}	0.39×10^{-2}	1.43×10^{-2}	-1.68
Stimulus Position	2.85×10^{-2}	-1.94×10^{-2}	7.64×10^{-2}	2.45×10^{-2}	1.17
Semantic Context x Presentation Number	$\mathbf{4.34 \times 10^{-2}}$	$\mathbf{0.97 \times 10^{-2}}$	$\mathbf{7.72 \times 10^{-2}}$	$\mathbf{1.72 \times 10^{-2}}$	**2.53**
B. Fixed effects of the logistic mixed effect model on accuracy rates					
	β raw	*CI (lower)*	*CI (upper)*	*SE*	*Wald Z*
Intercept	2.8	0.43	5.17	1.21	2.31
Semantic Context	1.15	-1.56	3.86	1.38	0.83
Presentation Number	0.28	-0.48	1.05	0.39	0.73
Stimulus Position	-0.08	-1.01	0.86	0.48	-0.16
Semantic Context x Presentation Number	-0.53	-1.34	0.29	0.42	-1.26

3. Stimulus-locked evolution of the effects of Structure and Window on HFB and tables with all fixed effects of the linear mixed effect models.

3.1. Frontal lobe results stimulus-locked

There were main effects of Structure (Wald $\chi2(3) = 120.79$, $p < .001$) and Window (Wald $\chi2(1) = 190.20$, $p < .001$), and an interaction between Structure and Window (Wald $\chi2(3) = 335.56$, $p < .001$): There was overall more HFB activity in the lateral PFC, medial M1/PMC, and medial PFC than in the lateral M1/PMC (Table S3). There was also more HFB activity the further away from stimulus onset and

this increase in activity was greater for the lateral M1/PMC than for the other frontal structures (Table S3).

Table S3: Fixed effects output of the mixed effect model for the frontal lobe in the stimulus-locked analyses: Beta coefficients (raw), confidence intervals for the beta coefficients (CI: lower and upper bound in log-scale), standard errors (SE), t-values for each of the fixed effects in the linear mixed effect model on trial-by-trial mean HFB. Effects reported in the main manuscript are in bold.

Fixed effects of the mixed effect model for the frontal lobe in the stimulus-locked analyses					
	β raw	*CI (lower)*	*CI (upper)*	*SE*	*t-Value*
(Intercept)	-2.133e+00	-4.70E+000	4.35E-001	1.310e+00	-1.628
Semantic Context	**1.623e+00**	**-1.53E-001**	**3.40E+000**	**9.062e-01**	**1.791**
Presentation Number	-8.356e-01	-1.61E+000	-6.11E-002	3.951e-01	-2.115
Structure (lateral PFC vs. lateral M1/PMC)	1.101e+01	8.91E+000	1.31E+001	1.069e+00	10.293
Structure (medial M1/PMC vs. lateral M1/PMC)	5.456e+00	1.77E+000	9.14E+000	1.880e+00	2.902
Structure (medial PFC vs. lateral M1/PMC)	4.217e+00	1.05E+000	7.39E+000	1.617e+00	2.608
Window	6.173e+00	5.30E+000	7.05E+000	4.476e-01	13.791
Stimulus Position	6.255e-02	-2.26E-001	3.51E-001	1.472e-01	0.425
Structure (lateral PFC vs. lateral M1/PMC) x Window	-5.425e+00	-6.01E+000	-4.84E+000	2.972e-01	-18.257
Structure (medial M1/PMC vs. lateral M1/PMC) x Window	-4.070e+00	-5.15E+000	-2.99E+000	5.504e-01	-7.394
Structure (medial PFC vs. lateral M1/PMC) x Window	-4.073e+00	-4.97E+000	-3.17E+000	4.589e-01	-8.876
Semantic Context x Presentation Number	-2.366e-01	-5.88E-001	1.15E-001	1.793e-01	-1.32
Semantic Context x Structure (lateral PFC vs. lateral M1/PMC)	-1.517e+00	-3.50E+000	4.71E-001	1.014e+00	-1.496
Semantic Context x Structure (medial M1/PMC vs. lateral M1/PMC)	-2.696e+00	-5.99E+000	5.96E-001	1.679e+00	-1.605
Semantic Context x Structure (medial PFC vs. lateral M1/PMC)	-1.784e-01	-3.17E+000	2.81E+000	1.525e+00	-0.117
Semantic Context x Window	**-5.267e-01**	**-1.01E+000**	**-4.21E-002**	**2.472e-01**	**-2.13**
Semantic Context x Structure (lateral PFC vs. lateral M1/PMC) x Window	**6.092e-01**	**5.47E-002**	**1.16E+000**	**2.829e-01**	**2.153**
Semantic Context x Structure (medial M1/PMC vs. lateral M1/PMC) x Window	**8.305e-01**	**-1.34E-001**	**1.80E+000**	**4.922e-01**	**1.687**
Semantic Context x Structure (medial PFC vs. lateral M1/PMC) x Window	**-2.339e-01**	**-1.08E+000**	**6.11E-001**	**4.310e-01**	**-0.543**

3.2. Temporal lobe results stimulus-locked

There was a main effect of Stimulus Position (Wald $\chi2(1) = 5.21$, $p = .022$), where stimuli

presented on the left of the fixation cross (i.e., in the ipsi-lateral visual field) were associated with lower HFB than stimuli presented on the right of the fixation cross (i.e., in the contra-lateral visual field, see Table S4). As in the frontal lobe model, there was a main effect of Structure (Wald $\chi2(3) = 120.10$, $p < .001$), and an interaction between Structure and Window (Wald $\chi2(3) = 139.98$, $p < .001$): There was overall less HFB activity in the STG and in the MTG than in the ITG, and more HFB activity in the ventral temporal lobe than in the ITG. There was also a significant decrease in HFB activity in the ventral temporal lobe compared to the ITG and an increase in the STG compared to the ITG.

Table S4: Fixed effects output of the mixed effect model for the temporal lobe in the stimulus-locked analyses: Beta coefficients (raw), confidence intervals for the beta coefficients (CI: lower and upper bound in log-scale), standard errors (SE), t-values for each of the fixed effects in the linear mixed effect model on trial-by-trial mean HFB. Effects reported in the main manuscript are in bold.

Fixed effects of the mixed effect model for the temporal lobe in the stimulus-locked analyses					
	β raw	*CI (lower)*	*CI (upper)*	*SE*	*t-Value*
(Intercept)	1.54E+001	9.55E+000	2.11E+001	2.96E+000	5.19
Semantic Context	-2.07E+000	-4.80E+000	6.71E-001	1.40E+000	-1.48
Presentation Number	-5.14E-001	-1.23E+000	2.02E-001	3.65E-001	-1.407
Structure (MTG vs. ITG)	-4.45E+000	-8.15E+000	-7.55E-001	1.89E+000	-2.36
Structure (STG vs. ITG)	-1.61E+001	-2.00E+001	-1.22E+001	1.99E+000	-8.077
Structure (Ventral vs. ITG)	6.45E+000	2.24E+000	1.07E+001	2.15E+000	3.005
Window	-4.48E-001	-2.82E+000	1.92E+000	1.21E+000	-0.37
Stimulus Position	-5.05E-001	-9.39E-001	-7.15E-002	2.21E-001	-2.283
Structure (MTG vs. ITG) x Window	1.66E-001	-9.77E-001	1.31E+000	5.83E-001	0.285
Structure (STG vs. ITG) x Window	3.90E+000	2.71E+000	5.09E+000	6.08E-001	6.423
Structure (Ventral vs. ITG) x Window	-3.70E+000	-5.09E+000	-2.30E+000	7.13E-001	-5.184
Semantic Context x Presentation Number	1.21E-001	-4.07E-001	6.49E-001	2.69E-001	0.449
Semantic Context x Structure (MTG vs. ITG)	2.24E+000	-9.37E-001	5.41E+000	1.62E+000	1.381
Semantic Context x Structure (STG vs. ITG)	2.64E+000	-5.94E-001	5.88E+000	1.65E+000	1.6
Semantic Context x Structure (Ventral vs. ITG)	1.52E-001	-3.84E+000	4.14E+000	2.03E+000	0.075
Semantic Context x Window	**1.33E+000**	**3.92E-001**	**2.26E+000**	**4.76E-001**	**2.784**
Semantic Context x Structure (MTG vs. ITG) x Window	**-1.57E+000**	**-2.59E+000**	**-5.59E-001**	**5.18E-001**	**-3.04**
Semantic Context x Structure (STG vs. ITG) x Window	**-1.60E+000**	**-2.63E+000**	**-5.78E-001**	**5.23E-001**	**-3.063**
Semantic Context x Structure (Ventral vs. ITG) x Window	**-8.84E-001**	**-2.23E+000**	**4.63E-001**	**6.87E-001**	**-1.286**

4. Response-locked evolution of the effects of Structure and Window on HFB.

4.1. **Frontal lobe results response-locked**

There were main effects of Structure (Wald $\chi2(3) = 65.94$, $p < .001$): Mean HFB was greater in the lateral PFC than in the lateral M1/PMC (Table S5). There was also a main effect of Window (Wald $\chi2(1) = 38.44$, $p < .001$): HFB increased the closer to vocal onset. Finally, there was an interaction between Structure and Window (Wald $\chi2(3) = 321.17$, $p < .001$), which was due to a larger HFB increase in the lateral M1/PMC than in all the other structures under analysis.

Table S5: Fixed effects output of the mixed effect model for the frontal lobe in the response-locked analyses: Beta coefficients (raw), confidence intervals for the beta coefficients (CI: lower and upper bound in log-scale), standard errors (SE), t-values for each of the fixed effects in the linear mixed effect model on trial-by-trial mean HFB. Effects reported in the main manuscript are in bold.

Fixed effects of the mixed effect model for the frontal lobe in the response-locked analyses					
	β raw	*CI (lower)*	*CI (upper)*	*SE*	*t-Value*
(Intercept)	3.59E+000	-8.86E-002	7.27E+000	1.88E+000	1.913
Semantic Context	**1.85E+000**	**4.22E-001**	**3.28E+000**	**7.29E-001**	**2.539**
Presentation Number	-1.24E+000	-1.78E+000	-7.04E-001	2.74E-001	-4.527
Structure (lateral PFC vs. lateral M1/PMC)	5.45E+000	3.77E+000	7.14E+000	8.59E-001	6.347
Structure (medial M1/PMC vs. lateral M1/PMC)	1.09E+000	-2.25E+000	4.44E+000	1.71E+000	0.641
Structure (medial PFC vs. lateral M1/PMC)	-1.39E+000	-3.93E+000	1.14E+000	1.29E+000	-1.079
Window	5.21E+000	3.56E+000	6.86E+000	8.40E-001	6.2
Stimulus Position	1.73E-001	-9.34E-002	4.40E-001	1.36E-001	1.273
Structure (lateral PFC vs. lateral M1/PMC) x Window	-4.55E+000	-5.04E+000	-4.05E+000	2.54E-001	-17.875
Structure (medial M1/PMC vs. lateral M1/PMC) x Window	-3.15E+000	-4.17E+000	-2.14E+000	5.16E-001	-6.116
Structure (medial PFC vs. lateral M1/PMC) x Window	-3.16E+000	-3.94E+000	-2.38E+000	3.98E-001	-7.936
Semantic Context x Presentation Number	-1.40E-001	-4.64E-001	1.85E-001	1.66E-001	-0.844
Semantic Context x Structure (lateral PFC vs. lateral M1/PMC)	-7.00E-001	-2.33E+000	9.26E-001	8.30E-001	-0.843
Semantic Context x Structure (medial M1/PMC vs. lateral M1/PMC)	-1.31E+000	-4.45E+000	1.83E+000	1.60E+000	-0.818
Semantic Context x Structure (medial PFC vs. lateral M1/PMC)	-7.16E-001	-3.14E+000	1.71E+000	1.24E+000	-0.579
Semantic Context x Window	**-5.05E-001**	**-9.73E-001**	**-3.70E-002**	**2.39E-001**	**-2.115**

Semantic Context x Structure (lateral PFC vs. lateral M1/PMC) x Window	2.76E-001	-2.06E-001	7.58E-001	2.46E-001	1.124
Semantic Context x Structure (medial M1/PMC vs. lateral M1/PMC) x Window	2.46E-001	-7.06E-001	1.20E+000	4.86E-001	0.506
Semantic Context x Structure (medial PFC vs. lateral M1/PMC) x Window	2.00E-001	-5.46E-001	9.45E-001	3.81E-001	0.524

4.2. Temporal lobe results response-locked

Similar to what reported in the stimulus-locked analysis, there was a marginal effect of Stimulus Position (Wald $\chi2(1) = 3.63$, $p = .057$), where stimuli presented on the left of the fixation cross (i.e., in the ipsi-lateral visual field) were associated with lower HFB than stimuli presented on the right of the fixation cross (i.e., in the contra-lateral visual field). There was also a main effect of Structure (Wald $\chi2(3) = 10.69$, $p < .001$), and an interaction between Structure and Window (Wald $\chi2(3) = 17.46$, $p < .001$). There was overall more HFB in the ITG than in the STG. Mean HFB increased the closer to vocal-onset for the ITG and STG but not for the ventral temporal cortex where mean HFB tended to decrease the closer to vocal-onset (Table S6).

Table S6: Fixed effects output of the mixed effect model for the temporal lobe in the response-locked analyses: Beta coefficients (raw), confidence intervals for the beta coefficients (CI: lower and upper bound in log-scale), standard errors (SE), t-values for each of the fixed effects in the linear mixed effect model on trial-by-trial mean HFB. Effects reported in the main manuscript are in bold.

Fixed effects of the mixed effect model for the temporal lobe in the response-locked analyses					
	β raw	*CI (lower)*	*CI (upper)*	*SE*	*t-Value*
(Intercept)	1.813e+01	1.28E+001	2.35E+001	2.736e+00	6.626
Semantic Context	2.211e+00	-7.87E-001	5.21E+000	1.530e+00	1.445
Presentation Number	-8.129e-01	-2.06E+000	4.32E-001	6.350e-01	-1.28
Structure (MTG vs. ITG)	-7.402e+00	-1.11E+001	-3.68E+000	1.897e+00	-3.902
Structure (STG vs. ITG)	-1.800e+01	-2.19E+001	-1.41E+001	2.008e+00	-8.967
Structure (Ventral vs. ITG)	5.038e+00	8.71E-001	9.20E+000	2.126e+00	2.37
Window	5.819e-02	-2.00E+000	2.12E+000	1.051e+00	0.055
Stimulus Position	-4.360e-01	-8.81E-001	9.32E-003	2.272e-01	-1.919
Structure (MTG vs. ITG) x Window	-5.565e-01	-1.73E+000	6.15E-001	5.978e-01	-0.931
Structure (STG vs. ITG) x Window	3.783e+00	2.54E+000	5.02E+000	6.325e-01	5.981
Structure (Ventral vs. ITG) x Window	-4.682e+00	-6.04E+000	-3.32E+000	6.945e-01	-6.742
Semantic Context x Presentation Number	3.165e-01	-2.27E-001	8.60E-001	2.773e-01	1.141
Semantic Context x Structure (MTG vs. ITG)	-3.236e+00	-6.57E+000	9.63E-002	1.700e+00	-1.903

Semantic Context x Structure (STG vs. ITG)	-2.387e+00	-5.92E+000	1.15E+000	1.804e+00	-1.323
Semantic Context x Structure (Ventral vs. ITG)	-3.281e+00	-7.28E+000	7.20E-001	2.041e+00	-1.607
Semantic Context x Window	1.849e-01	-8.28E-001	1.20E+000	5.169e-01	0.358
Semantic Context x Structure (MTG vs. ITG) x Window	-2.238e-01	-1.30E+000	8.51E-001	5.484e-01	-0.408
Semantic Context x Structure (STG vs. ITG) x Window	2.226e-01	-8.86E-001	1.33E+000	5.656e-01	0.394
Semantic Context x Structure (Ventral vs. ITG) x Window	-2.525e-01	-1.57E+000	1.07E+000	6.740e-01	-0.375

5. HFB-RT correlation results

5.1. **Frontal lobe**

Table S7: Fixed effects output of the mixed effect models for the frontal lobe in the stimulus-locked (A) and response-locked analyses of HFB-RT correlation coefficients: Beta coefficients (raw), confidence intervals for the beta coefficients (CI: lower and upper bound in log-scale), standard errors (SE), t-values for each of the fixed effects in the linear mixed effect model. Effects reported in the main manuscript are in bold.

A. Fixed effects of the mixed effect model for the frontal lobe in the stimulus-locked analyses

	β raw	*CI (lower)*	*CI (upper)*	*SE*	*t-Value*
(Intercept)	-5.61E-002	-1.14E-001	1.93E-003	2.96E-002	-1.895
Structure (lateral PFC vs. lateral M1/PMC)	3.86E-002	-7.20E-002	1.49E-001	5.64E-002	0.684
Structure (medial M1/PMC vs. lateral M1/PMC)	1.24E-001	-5.16E-002	3.00E-001	8.98E-002	1.386
Structure (medial PFC vs. lateral M1/PMC)	-8.37E-003	-1.60E-001	1.43E-001	7.71E-002	-0.109
Window	1.84E-002	-4.89E-003	4.16E-002	1.19E-002	1.548
Structure (lateral PFC vs. lateral M1/PMC) x Window	-3.75E-002	-6.86E-002	-6.30E-003	1.59E-002	-2.356
Structure (medial M1/PMC vs. lateral M1/PMC) x Window	-1.17E-002	-6.56E-002	4.22E-002	2.75E-002	-0.426
Structure (medial PFC vs. lateral M1/PMC) x Window	4.63E-003	-3.91E-002	4.84E-002	2.23E-002	0.207

B. Fixed effects of the mixed effect model for the frontal lobe in the response-locked analyses

	β raw	*CI (lower)*	*CI (upper)*	*SE*	*t-Value*
(Intercept)	1.77E-001	6.17E-002	2.92E-001	5.86E-002	3.011
Structure (lateral PFC vs. lateral M1/PMC)	**1.02E-001**	**1.39E-002**	**1.91E-001**	**4.52E-002**	**2.268**
Structure (medial M1/PMC vs. lateral M1/PMC)	**1.83E-001**	**1.12E-002**	**3.55E-001**	**8.77E-002**	**2.088**
Structure (medial PFC vs. lateral M1/PMC)	**-2.35E-002**	**-1.44E-001**	**9.75E-002**	**6.17E-002**	**-0.38**
Window	**-5.33E-002**	**-8.14E-002**	**-2.52E-002**	**1.44E-002**	**-3.714**

Structure (lateral PFC vs. lateral M1/PMC) x Window	**-1.76E-002**	**-4.35E-002**	**8.41E-003**	**1.33E-002**	**-1.325**
Structure (medial M1/PMC vs. lateral M1/PMC) x Window	**-3.49E-002**	**-8.64E-002**	**1.65E-002**	**2.63E-002**	**-1.33**
Structure (medial PFC vs. lateral M1/PMC) x Window	**3.05E-002**	**-6.93E-003**	**6.80E-002**	**1.91E-002**	**1.597**

5.2. **Temporal lobe**

Stimulus-locked, HFB-RT correlations only tended to become more positive the further away from stimulus-onset (*Wald* $\chi^2(1) = 3.65$, $p = 0.056$; Figure S7A and S8A). There was an interaction between Structure and Window (*Wald* $\chi^2(3) = 30.58$, $p < 0.001$) but however, in contrast with the evolution of the semantic context effects, this was due to the fact only the STG showed the opposite pattern: in the STG, HFB-RT correlations became more negative the further away from stimulus-onset (Table S8A). There was also a main effect of Structure on HFB-RT correlations: HFB-RT correlations were overall more negative in the STG than in the other structures stimulus-locked (*Wald* $\chi^2(3) = 17.74$, $p < 0.001$, Table S8A).

Response-locked, there was only a marginal effect of Structure (*Wald* $\chi^2(3) = 7.32$, $p = 0.062$), HFB-RT correlations were overall more negative in the MTG than in the other temporal lobe structures (Table S8B).

Table S8: Fixed effects output of the mixed effect models for the temporal lobe in the stimulus-locked (A) and response-locked analyses of HFB-RT correlation coefficients: Beta coefficients (raw), confidence intervals for the beta coefficients (CI: lower and upper bound in log-scale), standard errors (SE), t-values for each of the fixed effects in the linear mixed effect model. Effects reported in the main manuscript are in bold.

A. Fixed effects of the mixed effect model for the temporal lobe in the stimulus-locked analyses

	β raw	*CI (lower)*	*CI (upper)*	*SE*	*t-Value*
(Intercept)	-1.95E-001	-3.65E-001	-2.41E-002	8.70E-002	-2.237
Structure (MTG vs. ITG)	4.23E-002	-1.28E-001	2.13E-001	8.69E-002	0.487
Structure (STG vs. ITG)	2.71E-001	9.49E-002	4.47E-001	8.97E-002	3.017
Structure (Ventral vs. ITG)	-5.76E-002	-2.68E-001	1.52E-001	1.07E-001	-0.538
Window	6.64E-002	-1.69E-003	1.35E-001	3.48E-002	1.911
Structure (MTG vs. ITG) x Window	-2.67E-002	-8.16E-002	2.81E-002	2.80E-002	-0.955
Structure (STG vs. ITG) x Window	-1.13E-001	-1.69E-001	-5.63E-002	2.88E-002	-3.918
Structure (Ventral vs. ITG) x Window	3.63E-002	-3.49E-002	1.07E-001	3.63E-002	0.999

B. Fixed effects of the mixed effect model for the temporal lobe in the response-locked analyses

	β raw	*CI (lower)*	*CI (upper)*	*SE*	*t-Value*
(Intercept)	1.02E-001	-1.00E-001	3.03E-001	1.03E-001	0.987
Structure (MTG vs. ITG)	-1.62E-001	-3.56E-001	3.14E-002	9.89E-002	-1.642
Structure (STG vs. ITG)	2.69E-002	-1.76E-001	2.30E-001	1.04E-001	0.260
Structure (Ventral vs. ITG)	-1.05E-001	-3.27E-001	1.17E-001	1.13E-001	-0.926
Window	-4.34E-002	-1.03E-001	1.57E-002	3.02E-002	-1.439
Structure (MTG vs. ITG) x Window	5.16E-002	-8.52E-003	1.12E-001	3.07E-002	1.682
Structure (STG vs. ITG) x Window	1.39E-002	-4.82E-002	7.60E-002	3.17E-002	0.438
Structure (Ventral vs. ITG) x Window	2.51E-002	-4.69E-002	9.71E-002	3.67E-002	0.683

6. Fronto-temporal mean HFB trial-by-trial non-significant correlation results in ST32

Stimulus-locked:

13. between 0 and 400 ms post-stimulus: medial PFC vs. ITG: rho= -0.044, p_{corr} = 1; medial M1/PMC vs. ITG: rho= 0.092, p_{corr} = 1; lateral M1/PMC vs. ITG: rho= 0.027, p_{corr} = 1.
14. between 400 and 1000 ms post-stimulus: medial PFC vs. ITG: rho= 0.197, p_{corr} = .211; medial M1/PMC vs. ITG: rho= 0.179, p_{corr} = .158.

Response-locked:

-750 and -350 ms pre vocal-onset: Medial M1/PMC and ITG : rho= 0.152, p_{corr} = .091

7. ERP analysis

We conducted ERP analysis on the present data to test whether or not a similar pattern as the one we described on the HFB activity was visible on ERPs and whether or not findings with intracranial ERPs could be related to findings with surface ERPs in this paradigm.

Methods and Results

In order to compute the ERPs, the raw signal for each electrode was bandpass filtered between 0.1 and 100 Hz using a flat gaussian filter. In order to be able to directly compare the HFB results to the ERP results, we used a similar criteria for ERP detection as for HFB detection expect we used two-way student t-tests to do the ERP amplitude comparisons given negative ERPs are well-documented in the field (e.g. N100, N200, N400). An electrode was considered "active" if it had at least one 100-ms-long segment which had significant HFB power after FDR correction (as in [39]).

We found that around the same number of electrodes showed significant ERPs (in average 33, σ = 21 stimulus-locked, and in average 38, σ = 23 response-locked) and HFB (in average 37, σ = 9 stimulus-locked, and in average 44, σ = 11 response-locked; there was no significant difference between the number of electrodes showing ERPs and HFB stimulus or response-locked, ts<1). However, there was less than

40% overlap between the recording sites showing HFB and those showing ERPs across patients (stimulus-locked average: 39%, σ = 11%; response-locked average: 36%, σ = 14%, Figure S10).

We performed the same models stimulus and response-locked for the frontal and temporal lobes as for the analysis of the HFB power.

There was no significant effect of context or any interaction between context and the other factors under analysis in the models we performed (Table S9), except for a triple interaction between Semantic Context, Structure and Window in the frontal lobe model response locked (*Wald* $\chi^2(3) = 7.92$, $p = 0.048$): in all structures but the lateral PFC, overall ERP amplitude became more negative in HOM versus HET blocks the closer to vocal onset.

Table S9: Fixed effects output of the mixed effect models for the stimulus and response-locked analyses of the ERPs: Beta coefficients (raw), confidence intervals for the beta coefficients (CI: lower and upper bounds), standard errors (SE), t-values for each of the fixed effects in the linear mixed effect model on trial-by-trial mean ERPs. Significant effects are in bold.

A. Fixed effects of the mixed effect model on ERP amplitude for the frontal lobe in the stimulus-locked analyses

	β raw	*CI (lower)*	*CI (upper)*	*SE*	*t-Value*
(Intercept)	4.29E+000	-1.37E+000	9.95E+000	2.89E+000	1.485
Semantic Context	1.29E+000	-9.15E-001	3.49E+000	1.12E+000	1.145
Presentation Number	4.39E-001	-6.14E-001	1.49E+000	5.38E-001	0.817
Structure (lateral PFC vs. lateral M1/PMC)	**-6.21E+000**	**-8.84E+000**	**-3.57E+000**	**1.34E+000**	**-4.616**
Structure (medial M1/PMC vs. lateral M1/PMC)	7.15E+000	-4.52E+000	1.88E+001	5.95E+000	1.201
Structure (medial PFC vs. lateral M1/PMC)	-1.25E+000	-8.15E+000	5.64E+000	3.52E+000	-0.357
Window	2.58E-001	-1.27E+000	1.79E+000	7.82E-001	0.33
Stimulus Position	**7.09E-001**	**2.97E-001**	**1.12E+000**	**2.10E-001**	**3.375**
Structure (lateral PFC vs. lateral M1/PMC) x Window	**-2.27E+000**	**-3.07E+000**	**-1.46E+000**	**4.09E-001**	**-5.539**
Structure (medial M1/PMC vs. lateral M1/PMC) x Window	**-5.67E+000**	**-8.88E+000**	**-2.47E+000**	**1.64E+000**	**-3.469**
Structure (medial PFC vs. lateral M1/PMC) x Window	**-4.12E+000**	**-6.27E+000**	**-1.97E+000**	**1.10E+000**	**-3.755**
Semantic Context x Presentation Number	3.65E-001	-1.39E-001	8.68E-001	2.57E-001	1.42
Semantic Context x Structure (lateral PFC vs. lateral M1/PMC)	-2.83E+000	-5.33E+000	-3.26E-001	1.28E+000	-2.216
Semantic Context x Structure (medial M1/PMC vs. lateral M1/PMC)	-2.97E+000	-1.43E+001	8.31E+000	5.76E+000	-0.516
Semantic Context x Structure (medial PFC vs. lateral M1/PMC)	-1.64E+000	-8.13E+000	4.85E+000	3.31E+000	-0.494
Semantic Context x Window	-4.48E-001	-1.12E+000	2.24E-001	3.43E-001	-1.307
Semantic Context x Structure (lateral PFC vs. lateral M1/PMC) x Window	1.03E+000	2.63E-001	1.79E+000	3.89E-001	2.635
Semantic Context x Structure (medial M1/PMC vs. lateral M1/PMC) x Window	6.29E-001	-2.46E+000	3.71E+000	1.57E+000	0.399
Semantic Context x Structure (medial PFC vs. lateral M1/PMC) x Window	3.62E-001	-1.67E+000	2.39E+000	1.04E+000	0.35

B. Fixed effects of the mixed effect model on ERP amplitude for the temporal lobe in the stimulus-locked analyses

	β raw	*CI (lower)*	*CI (upper)*	*SE*	*t-Value*
(Intercept)	4.66E+001	7.00E-001	9.26E+001	2.34E+001	1.99
Semantic Context	2.10E+001	-3.37E+000	4.55E+001	1.25E+001	1.689
Presentation Number	-1.28E-001	-4.76E+000	4.51E+000	2.37E+000	-0.054
Structure (MTG vs. ITG)	**-4.27E+001**	**-7.06E+001**	**-1.48E+001**	**1.43E+001**	**-2.995**
Structure (STG vs. ITG)	**-4.54E+001**	**-7.36E+001**	**-1.71E+001**	**1.44E+001**	**-3.15**
Structure (Ventral vs. ITG)	-3.21E+001	-8.34E+001	1.93E+001	2.62E+001	-1.224
Window	-1.03E+001	-2.47E+001	4.23E+000	7.39E+000	-1.388
Stimulus Position	**-3.54E+000**	**-6.73E+000**	**-3.42E-001**	**1.63E+000**	**-2.17**
Structure (MTG vs. ITG) x Window	5.81E+000	-3.28E+000	1.49E+001	4.64E+000	1.253
Structure (STG vs. ITG) x Window	5.46E+000	-3.73E+000	1.46E+001	4.68E+000	1.165
Structure (Ventral vs. ITG) x Window	5.31E+000	-1.01E+001	2.07E+001	7.86E+000	0.675
Semantic Context x Presentation Number	2.88E+000	-2.42E+000	8.18E+000	2.70E+000	1.066
Semantic Context x Structure (MTG vs. ITG)	-1.27E+001	-4.02E+001	1.48E+001	1.40E+001	-0.907
Semantic Context x Structure (STG vs. ITG)	-2.15E+001	-4.84E+001	5.43E+000	1.37E+001	-1.564
Semantic Context x Structure (Ventral vs. ITG)	-1.88E+001	-6.44E+001	2.67E+001	2.32E+001	-0.811
Semantic Context x Window	-4.07E+000	-1.21E+001	3.92E+000	4.08E+000	-0.998
Semantic Context x Structure (MTG vs. ITG) x Window	2.99E+000	-5.88E+000	1.19E+001	4.53E+000	0.66
Semantic Context x Structure (STG vs. ITG) x Window	3.67E+000	-5.02E+000	1.24E+001	4.44E+000	0.828
Semantic Context x Structure (Ventral vs. ITG) x Window	3.87E+000	-1.02E+001	1.80E+001	7.19E+000	0.539

C. Fixed effects of the mixed effect model on ERP amplitude for the frontal lobe in the response-locked analyses

	β raw	*CI (lower)*	*CI (upper)*	*SE*	*t-Value*
(Intercept)	9.04E+000	2.51E+000	1.56E+001	3.33E+000	2.713
Semantic Context	-5.65E-001	-3.63E+000	2.50E+000	1.56E+000	-0.361
Presentation Number	2.78E-001	-4.99E-001	1.05E+000	3.96E-001	0.7
Structure (lateral PFC vs. lateral M1/PMC)	**-1.96E+001**	**-2.30E+001**	**-1.62E+001**	**1.75E+000**	**-11.168**
Structure (medial M1/PMC vs. lateral M1/PMC)	-1.18E+001	-2.44E+001	7.55E-001	6.43E+000	-1.843
Structure (medial PFC vs. lateral M1/PMC)	-8.86E+000	-1.91E+001	1.34E+000	5.21E+000	-1.702
Window	-1.02E+000	-2.63E+000	5.79E-001	8.18E-001	-1.252
Stimulus Position	**1.30E+000**	**7.67E-001**	**1.84E+000**	**2.74E-001**	**4.756**
Structure (lateral PFC vs. lateral M1/PMC) x Window	**1.25E+000**	**2.49E-001**	**2.25E+000**	**5.10E-001**	**2.449**
Structure (medial M1/PMC vs. lateral M1/PMC) x Window	-6.86E-001	-4.36E+000	2.99E+000	1.88E+000	-0.365
Structure (medial PFC vs. lateral M1/PMC) x Window	-1.86E+000	-5.04E+000	1.32E+000	1.62E+000	-1.145
Semantic Context x Presentation Number	4.14E-001	-2.43E-001	1.07E+000	3.35E-001	1.236
Semantic Context x Structure (lateral PFC vs. lateral M1/PMC)	-1.56E+000	-4.88E+000	1.77E+000	1.69E+000	-0.919
Semantic Context x Structure (medial M1/PMC vs. lateral M1/PMC)	2.61E+000	-9.13E+000	1.43E+001	5.99E+000	0.435

Semantic Context x Structure (medial PFC vs. lateral M1/PMC)	-2.27E+000	-1.14E+001	6.85E+000	4.66E+000	-0.488
Semantic Context x Window	-4.48E-001	-1.33E+000	4.38E-001	4.52E-001	-0.992
Semantic Context x Structure (lateral PFC vs. lateral M1/PMC) x Window	**1.29E+000**	**3.34E-001**	**2.24E+000**	**4.87E-001**	**2.645**
Semantic Context x Structure (medial M1/PMC vs. lateral M1/PMC) x Window	-6.74E-001	-4.14E+000	2.79E+000	1.77E+000	-0.382
Semantic Context x Structure (medial PFC vs. lateral M1/PMC) x Window	7.77E-001	-2.15E+000	3.71E+000	1.50E+000	0.52

D. Fixed effects of the mixed effect model on ERP amplitude for the temporal lobe in the response-locked analyses

	β raw	*CI (lower)*	*CI (upper)*	*SE*	*t-Value*
(Intercept)	6.17E+001	1.39E+001	1.09E+002	2.44E+001	2.531
Semantic Context	1.03E+001	-1.88E+001	3.94E+001	1.48E+001	0.695
Presentation Number	-5.59E+000	-1.99E+001	8.68E+000	7.28E+000	-0.768
Structure (MTG vs. ITG)	**-7.44E+001**	**-1.08E+002**	**-4.06E+001**	**1.73E+001**	**-4.309**
Structure (STG vs. ITG)	**-6.65E+001**	**-1.00E+002**	**-3.30E+001**	**1.71E+001**	**-3.885**
Structure (Ventral vs. ITG)	-6.30E+001	-1.60E+002	3.39E+001	4.94E+001	-1.275
Window	-2.03E+001	-3.80E+001	-2.63E+000	9.01E+000	-2.252
Stimulus Position	-2.93E+000	-6.98E+000	1.11E+000	2.06E+000	-1.421
Structure (MTG vs. ITG) x Window	**1.43E+001**	**3.82E+000**	**2.48E+001**	**5.34E+000**	**2.675**
Structure (STG vs. ITG) x Window	**1.94E+001**	**9.13E+000**	**2.97E+001**	**5.24E+000**	**3.703**
Structure (Ventral vs. ITG) x Window	1.55E+001	-1.14E+001	4.25E+001	1.38E+001	1.13
Semantic Context x Presentation Number	-3.50E+000	-8.44E+000	1.43E+000	2.52E+000	-1.39
Semantic Context x Structure (MTG vs. ITG)	-2.54E+000	-3.58E+001	3.07E+001	1.69E+001	-0.15
Semantic Context x Structure (STG vs. ITG)	-1.38E+001	-4.62E+001	1.87E+001	1.65E+001	-0.832
Semantic Context x Structure (Ventral vs. ITG)	-1.60E+001	-1.09E+002	7.72E+001	4.76E+001	-0.337
Semantic Context x Window	-3.48E+000	-1.24E+001	5.49E+000	4.58E+000	-0.76
Semantic Context x Structure (MTG vs. ITG) x Window	2.29E+000	-7.93E+000	1.25E+001	5.21E+000	0.438
Semantic Context x Structure (STG vs. ITG) x Window	4.69E+000	-5.07E+000	1.44E+001	4.98E+000	0.941
Semantic Context x Structure (Ventral vs. ITG) x Window	5.43E+000	-2.07E+001	3.15E+001	1.33E+001	0.408

8. HFB analysis with 1st presentation included

We performed the same mixed-effect model analyses as reported in the main manuscript for the HFB power but including the data corresponding to the first presentation of the stimuli. Indeed, some studies have reported semantic priming for the first presentation of the stimuli (e.g., 30), however the presence of this effect has been shown to be variable (e.g., 30; 31) and so we did not include these analyses in the main manuscript.

8.1. Behavioral results

There was a main effect of Presentation Number on log-transformed naming latencies (Wald $\chi2(1) = 10.81$, $p = .001$): participants were faster with increasing repetitions, revealing a repetition effect (see Table S10 A for βraw, CI, SE, and t-values). However, there was no main effect of Semantic Context (Wald $\chi2(1) = 2.28$, $p = .131$). Finally, there was an interaction between Semantic Context and Presentation

Number (Wald $\chi2(1) = 8.67$, $p = .003$): with increasing repetitions, naming latencies increased in HOM vs. HET blocks.

There was a marginal effect of Presentation Number on accuracy rates (Wald $\chi2(1) = 2.96$, $p = .085$): participants tended to make less errors with increasing repetitions. As for reaction time data, there was no main effect of Semantic Context on accuracy rates (Wald $\chi2(1) = 0.28$, $p = .596$) but there was a significant interaction between Semantic Context and Presentation Number (Wald $\chi2(1) = 4.00$, $p = .045$, see Table S10 B for βraw, CI, SE, and t-values).

Table S10: Fixed effects output of the mixed effect models including the first presentation of the stimuli on naming latencies (A) and accuracy rates (B): Beta coefficients (raw, in log-scale), confidence intervals for the beta coefficients (CI: lower and upper bound in log-scale), standard errors (SE), t (for naming latencies) and Z (for accuracy rates) -values for each of the fixed effects in the mixed effect models. Significant effects are in bold.

A. Fixed effects of the mixed effect model on log-transformed naming latencies					
	β raw	*CI (lower)*	*CI (upper)*	*SE*	*t-Value*
Intercept	6.80	6.64	6.96	8.16×10^{-2}	83.28
Semantic Context	4.15×10^{-2}	-1.23×10^{-2}	9.53×10^{-2}	2.75×10^{-2}	1.51
Presentation Number	$\mathbf{-3.40 \times 10^{-2}}$	$\mathbf{-5.43 \times 10^{-2}}$	$\mathbf{-1.37 \times 10^{-2}}$	$\mathbf{1.03 \times 10^{-2}}$	**-3.29**
Stimulus Position	2.29×10^{-2}	-2.53×10^{-2}	7.11×10^{-2}	2.46×10^{-2}	0.93
Semantic Context x Presentation Number	$\mathbf{3.49 \times 10^{-2}}$	$\mathbf{1.67 \times 10^{-2}}$	$\mathbf{5.81 \times 10^{-2}}$	$\mathbf{1.19 \times 10^{-2}}$	**2.95**
B. Fixed effects of the logistic mixed effect model on accuracy rates					
	β raw	*CI (lower)*	*CI (upper)*	*SE*	*Wald Z*
Intercept	3.57	2.22	4.91	0.69	5.20
Semantic Context	-0.35	-1.62	0.93	0.65	-0.53
Presentation Number	0.46	-0.06	0.99	0.27	1.72
Stimulus Position	0.17	-0.51	0.86	0.35	0.49
Semantic Context x Presentation Number	-0.54	-1.08	-0.01	0.27	-2.00

8.2. ECoG results with 1st presentation included

8.2.1. Stimulus-locked results of the linear mixed effect models

In the temporal lobe, there was a marginal main effect of Semantic Context (Wald $\chi2(1) = 2.75$, $p = .097$): there tended to be overall more HFB power in HET vs. HOM blocks. There was also a significant interaction between Semantic Context and Window (Wald $\chi2(1) = 9.78$, $p = .002$): semantic interference

increased the further away from stimulus onset (Table S11). As in the analysis excluding the 1st presentation of the stimuli, there was also a 3-way interaction between Semantic Context, Window, and Structure (Wald $\chi2(3) = 13.73$, $p = .003$). There was also a main effect of Presentation Number (Wald $\chi2(1) = 5.14$, $p = .023$; HFB power decreased with increasing repetition), Structure (Wald $\chi2(3) = 191.99$, $p < .001$), Stimulus Position (Wald $\chi2(1) = 4.19$, $p = .041$), and an interaction between Structure and Window (Wald $\chi2(3) = 189.76$, $p < .001$). All these effects were in the same directions as those reported in the model performed without the 1st presentation of the stimuli.

Table S11: Fixed effects output of the mixed effect model for the temporal lobe in the stimulus-locked analysis with 1st presentation of the stimuli included: Beta coefficients (raw), confidence intervals for the beta coefficients (CI: lower and upper bound in log-scale), standard errors (SE), t-values for each of the fixed effects in the linear mixed effect model on trial-by-trial mean HFB. Values corresponding to significant effects are in bold.

	β raw	*CI (lower)*	*CI (upper)*	*SE*	*t-Value*
(Intercept)	1.53E+001	8.91E+000	2.16E+001	3.24E+000	4.708
Semantic Context	-2.16E+000	-4.71E+000	3.93E-001	1.30E+000	-1.658
Presentation Number	**-9.76E-001**	**-1.82E+000**	**-1.32E-001**	**4.31E-001**	**-2.266**
Structure (MTG vs. ITG)	**-3.98E+000**	**-7.10E+000**	**-8.63E-001**	**1.59E+000**	**-2.502**
Structure (STG vs. ITG)	**-1.66E+001**	**-1.98E+001**	**-1.33E+001**	**1.67E+000**	**-9.936**
Structure (Ventral vs. ITG)	**6.63E+000**	**3.00E+000**	**1.03E+001**	**1.85E+000**	**3.581**
Window	1.41E-001	-2.34E+000	2.62E+000	1.27E+000	0.112
Stimulus Position	**-3.97E-001**	**-7.77E-001**	**-1.70E-002**	**1.94E-001**	**-2.048**
Structure (MTG vs. ITG) x Window	-2.86E-001	-1.28E+000	7.03E-001	5.05E-001	-0.567
Structure (STG vs. ITG) x Window	**3.58E+000**	**2.55E+000**	**4.60E+000**	**5.22E-001**	**6.851**
Structure (Ventral vs. ITG) x Window	**-3.77E+000**	**-4.99E+000**	**-2.56E+000**	**6.22E-001**	**-6.07**
Semantic Context x Presentation Number	-5.35E-002	-3.97E-001	2.90E-001	1.76E-001	-0.305
Semantic Context x Structure (MTG vs. ITG)	2.40E+000	-4.64E-001	5.27E+000	1.46E+000	1.643
Semantic Context x Structure (STG vs. ITG)	**2.63E+000**	**-2.97E-001**	**5.56E+000**	**1.49E+000**	**1.762**
Semantic Context x Structure (Ventral vs. ITG)	-3.13E-001	-3.84E+000	3.21E+000	1.80E+000	-0.174
Semantic Context x Window	**1.43E+000**	**5.36E-001**	**2.33E+000**	**4.59E-001**	**3.128**
Semantic Context x Structure (MTG vs. ITG) x Window	**-1.56E+000**	**-2.48E+000**	**-6.40E-001**	**4.70E-001**	**-3.32**
Semantic Context x Structure (STG vs. ITG) x Window	**-1.56E+000**	**-2.49E+000**	**-6.26E-001**	**4.77E-001**	**-3.274**
Semantic Context x Structure (Ventral vs. ITG) x Window	-5.43E-001	-1.73E+000	6.49E-001	6.08E-001	-0.892

In the frontal lobe, there was no effect of Semantic Context or any interaction of Semantic Context with the other factors under comparison. This is in contrast with the analysis excluding the 1st presentation of the stimuli where an interaction of Semantic Context by Window and a 3-way interaction between Semantic Context, Window, and Structure were found (see main manuscript). We did find a main effect of Structure (Wald $\chi2(3) = 147.87$, $p < .001$), Window (Wald $\chi2(1) = 58.19$, $p < .001$), and an interaction

between Structure and Window (Wald $\chi2(3) = 425.62$, $p < .001$). These effects were in the same directions as those reported in the model performed without the 1st presentation of the stimuli (see Table S12).

Table S12: Fixed effects output of the mixed effect model for the frontal lobe in the stimulus-locked analysis with 1st presentation of the stimuli included: Beta coefficients (raw), confidence intervals for the beta coefficients (CI: lower and upper bound in log-scale), standard errors (SE), t-values for each of the fixed effects in the linear mixed effect model on trial-by-trial mean HFB. Values corresponding to significant effects are in bold.

Fixed effects of the mixed effect model for the frontal lobe in the stimulus-locked analyses

	β raw	*CI (lower)*	*CI (upper)*	*SE*	*t-value*
(Intercept)	-1.92E+000	-4.38E+000	5.48E-001	1.26E+000	-1.524
Semantic Context	7.97E-001	-2.54E+000	4.14E+000	1.70E+000	0.467
Presentation Number	-1.35E+000	-3.51E+000	8.06E-001	1.10E+000	-1.228
Structure (lateral PFC vs. lateral M1/PMC)	**1.08E+001**	**8.97E+000**	**1.27E+001**	**9.43E-001**	**11.468**
Structure (medial M1/PMC vs. lateral M1/PMC)	**6.27E+000**	**3.05E+000**	**9.49E+000**	**1.64E+000**	**3.814**
Structure (medial PFC vs. lateral M1/PMC)	**3.95E+000**	**1.16E+000**	**6.73E+000**	**1.42E+000**	**2.776**
Window	**6.39E+000**	**4.75E+000**	**8.03E+000**	**8.38E-001**	**7.628**
Stimulus Position	6.21E-002	-1.93E-001	3.17E-001	1.30E-001	0.477
Structure (lateral PFC vs. lateral M1/PMC) x Window	**-5.39E+000**	**-5.91E+000**	**-4.88E+000**	**2.62E-001**	**-20.562**
Structure (medial M1/PMC vs. lateral M1/PMC) x Window	**-4.03E+000**	**-4.98E+000**	**-3.09E+000**	**4.82E-001**	**-8.369**
Structure (medial PFC vs. lateral M1/PMC) x Window	**-4.28E+000**	**-5.07E+000**	**-3.49E+000**	**4.04E-001**	**-10.595**
Semantic Context x Presentation Number	-1.71E-001	-4.00E-001	5.83E-002	1.17E-001	-1.461
Semantic Context x Structure (lateral PFC vs. lateral M1/PMC)	-4.58E-001	-2.25E+000	1.33E+000	9.13E-001	-0.501
Semantic Context x Structure (medial M1/PMC vs. lateral M1/PMC)	-2.14E+000	-5.15E+000	8.72E-001	1.54E+000	-1.392
Semantic Context x Structure (medial PFC vs. lateral M1/PMC)	-7.36E-002	-2.76E+000	2.62E+000	1.37E+000	-0.054
Semantic Context x Window	-1.54E-001	-1.11E+000	8.03E-001	4.89E-001	-0.316
Semantic Context x Structure (lateral PFC vs. lateral M1/PMC) x Window	1.76E-001	-3.23E-001	6.74E-001	2.54E-001	0.691
Semantic Context x Structure (medial M1/PMC vs. lateral M1/PMC) x Window	2.92E-001	-5.86E-001	1.17E+000	4.48E-001	0.651
Semantic Context x Structure (medial PFC vs. lateral M1/PMC) x Window	-4.23E-001	-1.18E+000	3.36E-001	3.87E-001	-1.093

8.2.2. Response-locked results of the linear mixed effect models

In the temporal lobe, there was a main effect of Structure (Wald $\chi2(3) = 196.38$, $p < .001$). There was a marginal interaction between Semantic Context and Structure (Wald $\chi2(3) = 6.48$, $p = .090$), such that the context effect tended to decrease in the MTG vs. the ITG but not in comparison to the other structures; and an interaction between Structure and Window (Wald $\chi2(3) = 290.23$, $p < .001$; see Table S13 for statistical details).

Table S13: Fixed effects output of the mixed effect model for the temporal lobe in the response-locked analysis with 1st presentation of the stimuli included: Beta coefficients (raw), confidence intervals for the beta coefficients (CI: lower and upper bound in log-scale), standard errors (SE), t-values for each of the fixed effects in the linear mixed effect model on trial-by-trial mean HFB. Values corresponding to significant effects are in bold.

	β raw	*CI (lower)*	*CI (upper)*	*SE*	*t-value*
(Intercept)	2.06E+001	1.46E+001	2.66E+001	3.06E+000	6.751
Semantic Context	1.46E+000	-1.33E+000	4.25E+000	1.43E+000	1.024
Presentation Number	-1.32E+000	-2.94E+000	2.97E-001	8.25E-001	-1.601
Structure (MTG vs. ITG)	**-8.85E+000**	**-1.22E+001**	**-5.45E+000**	**1.73E+000**	**-5.104**
Structure (STG vs. ITG)	**-1.99E+001**	**-2.35E+001**	**-1.63E+001**	**1.82E+000**	**-10.916**
Structure (Ventral vs. ITG)	**4.69E+000**	**9.64E-001**	**8.42E+000**	**1.90E+000**	**2.467**
Window	-3.63E-001	-2.55E+000	1.83E+000	1.12E+000	-0.324
Stimulus Position	-2.43E-001	-6.41E-001	1.55E-001	2.03E-001	-1.196
Structure (MTG vs. ITG) x Window	-3.27E-001	-1.39E+000	7.39E-001	5.44E-001	-0.601
Structure (STG vs. ITG) x Window	**4.30E+000**	**3.17E+000**	**5.42E+000**	**5.73E-001**	**7.501**
Structure (Ventral vs. ITG) x Window	**-4.91E+000**	**-6.12E+000**	**-3.69E+000**	**6.21E-001**	**-7.904**
Semantic Context x Presentation Number	5.91E-002	-3.03E-001	4.21E-001	1.85E-001	0.32
Semantic Context x Structure (MTG vs. ITG)	**-3.64E+000**	**-6.66E+000**	**-6.21E-001**	**1.54E+000**	**-2.363**
Semantic Context x Structure (STG vs. ITG)	-1.82E+000	-4.99E+000	1.35E+000	1.62E+000	-1.125
Semantic Context x Structure (Ventral vs. ITG)	-1.40E+000	-4.99E+000	2.18E+000	1.83E+000	-0.766
Semantic Context x Window	5.15E-001	-4.50E-001	1.48E+000	4.93E-001	1.046
Semantic Context x Structure (MTG vs. ITG) x Window	-5.69E-002	-1.03E+000	9.16E-001	4.96E-001	-0.115
Semantic Context x Structure (STG vs. ITG) x Window	-7.43E-002	-1.08E+000	9.30E-001	5.12E-001	-0.145
Semantic Context x Structure (Ventral vs. ITG) x Window	-4.10E-001	-1.59E+000	7.73E-001	6.03E-001	-0.679

In the frontal lobe, there was only a marginal effect of Semantic Context (Wald $\chi2(1) = 3.21$, $p = .073$), whereas this effect was significant in the analysis excluding the 1st presentation of the stimuli. There were main effects of Presentation Number (Wald $\chi2(1) = 88.61$, $p < .001$), Structure (Wald $\chi2(3) = 82.84$, $p < .001$), and Window (Wald $\chi2(1) = 43.88$, $p < .001$, and an interaction between Structure and Window (Wald $\chi2(3) = 416.18$, $p < .001$). These effects were in the same directions as those reported in the model performed without the 1st presentation of the stimuli (see Table S14).

Table S14: Fixed effects output of the mixed effect model for the frontal lobe in the response-locked analysis with 1st presentation of the stimuli included: Beta coefficients (raw), confidence intervals for the beta coefficients (CI: lower and upper bound in log-scale), standard errors (SE), t-values for each of the fixed effects in the linear mixed effect model on trial-by-trial mean HFB. Values corresponding to significant effects are in bold.

Fixed effects of the mixed effect model for the frontal lobe in the stimulus-locked analyses

	β raw	*CI (lower)*	*CI (upper)*	*SE*	*t-value*
(Intercept)	4.36E+000	1.20E+000	7.52E+000	1.61E+000	2.701
Semantic Context	1.23E+000	-1.15E-001	2.58E+000	6.87E-001	1.793
Presentation Number	**-1.39E+000**	**-1.68E+000**	**-1.10E+000**	**1.48E-001**	**-9.414**
Structure (lateral PFC vs. lateral M1/PMC)	**5.54E+000**	**4.06E+000**	**7.03E+000**	**7.56E-001**	**7.329**
Structure (medial M1/PMC vs. lateral M1/PMC)	2.29E+000	-6.32E-001	5.20E+000	1.49E+000	1.536
Structure (medial PFC vs. lateral M1/PMC)	-1.14E+000	-3.36E+000	1.08E+000	1.13E+000	-1.008
Window	**5.16E+000**	**3.63E+000**	**6.69E+000**	**7.79E-001**	**6.624**
Stimulus Position	1.56E-001	-7.95E-002	3.91E-001	1.20E-001	1.297
Structure (lateral PFC vs. lateral M1/PMC) x Window	**-4.57E+000**	**-5.01E+000**	**-4.13E+000**	**2.25E-001**	**-20.348**
Structure (medial M1/PMC vs. lateral M1/PMC) x Window	**-3.20E+000**	**-4.08E+000**	**-2.31E+000**	**4.52E-001**	**-7.072**
Structure (medial PFC vs. lateral M1/PMC) x Window	**-3.03E+000**	**-3.71E+000**	**-2.34E+000**	**3.50E-001**	**-8.651**
Semantic Context x Presentation Number	1.37E-001	-7.42E-002	3.49E-001	1.08E-001	1.273
Semantic Context x Structure (lateral PFC vs. lateral M1/PMC)	-1.26E-001	-1.58E+000	1.33E+000	7.43E-001	-0.17
Semantic Context x Structure (medial M1/PMC vs. lateral M1/PMC)	-1.69E+000	-4.50E+000	1.12E+000	1.43E+000	-1.181
Semantic Context x Structure (medial PFC vs. lateral M1/PMC)	-2.78E-001	-2.43E+000	1.88E+000	1.10E+000	-0.253
Semantic Context x Window	-2.94E-001	-6.94E-001	1.06E-001	2.04E-001	-1.44
Semantic Context x Structure (lateral PFC vs. lateral M1/PMC) x Window	3.39E-002	-3.93E-001	4.60E-001	2.18E-001	0.156
Semantic Context x Structure (medial M1/PMC vs. lateral M1/PMC) x Window	1.95E-001	-6.35E-001	1.03E+000	4.24E-001	0.46
Semantic Context x Structure (medial PFC vs. lateral M1/PMC) x Window	2.17E-002	-6.31E-001	6.74E-001	3.33E-001	0.065

Supplementary figures

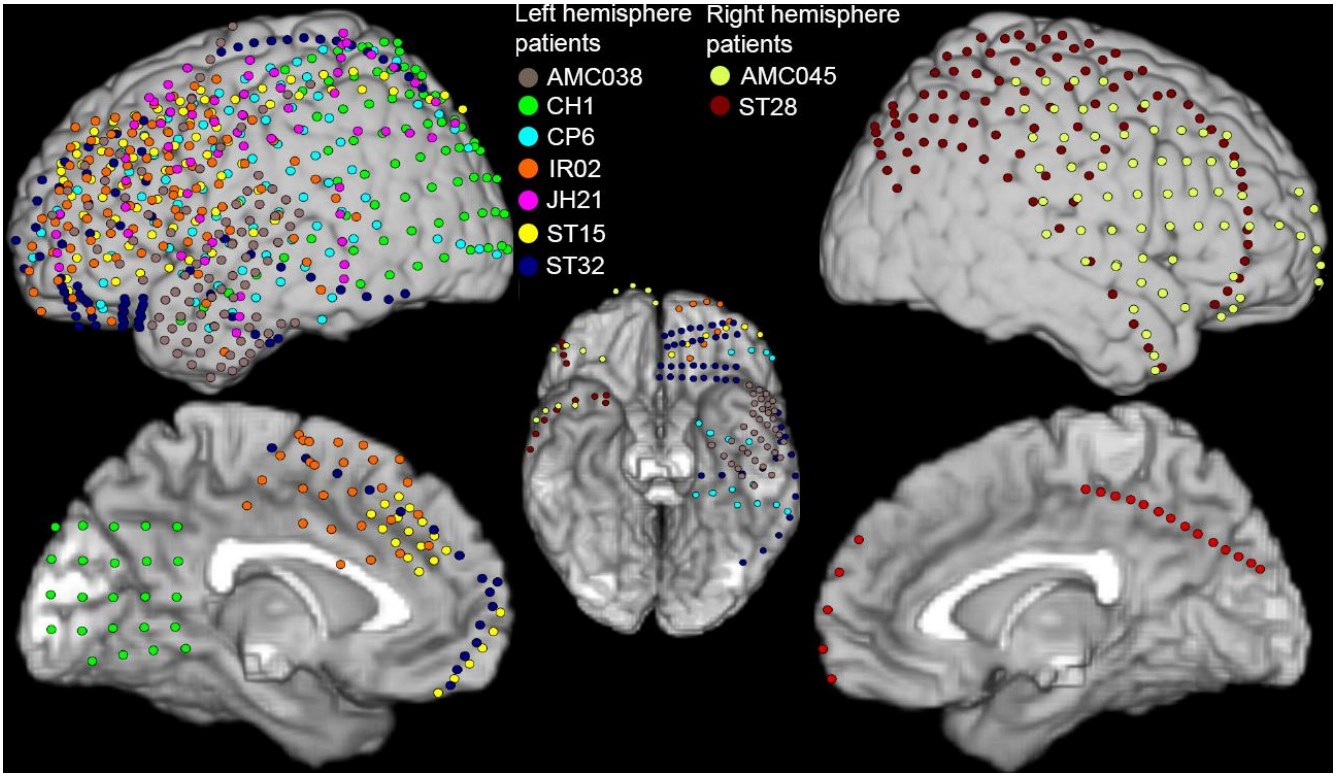

Figure S1: Electrode coverage for all patients who participated in the study in MNI space (all electrodes are represented). Each color represents the electrodes for a different patient. More extensive coverage over the frontal, temporal, and occipital was obtained for the left than right hemisphere.

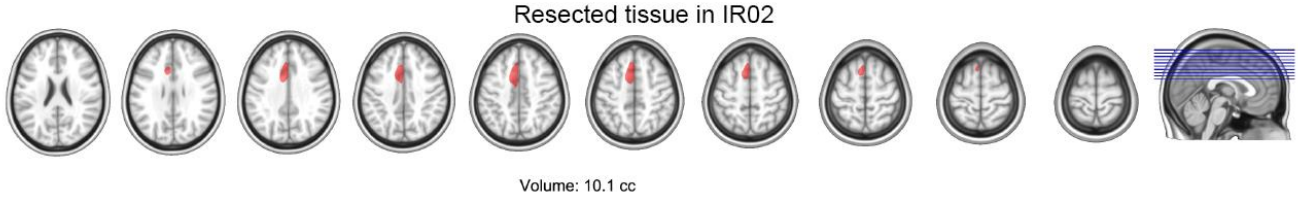

Figure S2: Reconstruction of the resected area in patient IR02 on horizontal slices of this patient's brain. This patient had an abnormally large semantic interference effect prior to resection as described in the text, indicating abnormal tissue in this area leads to a massive increase of the semantic interference effect in picture naming.

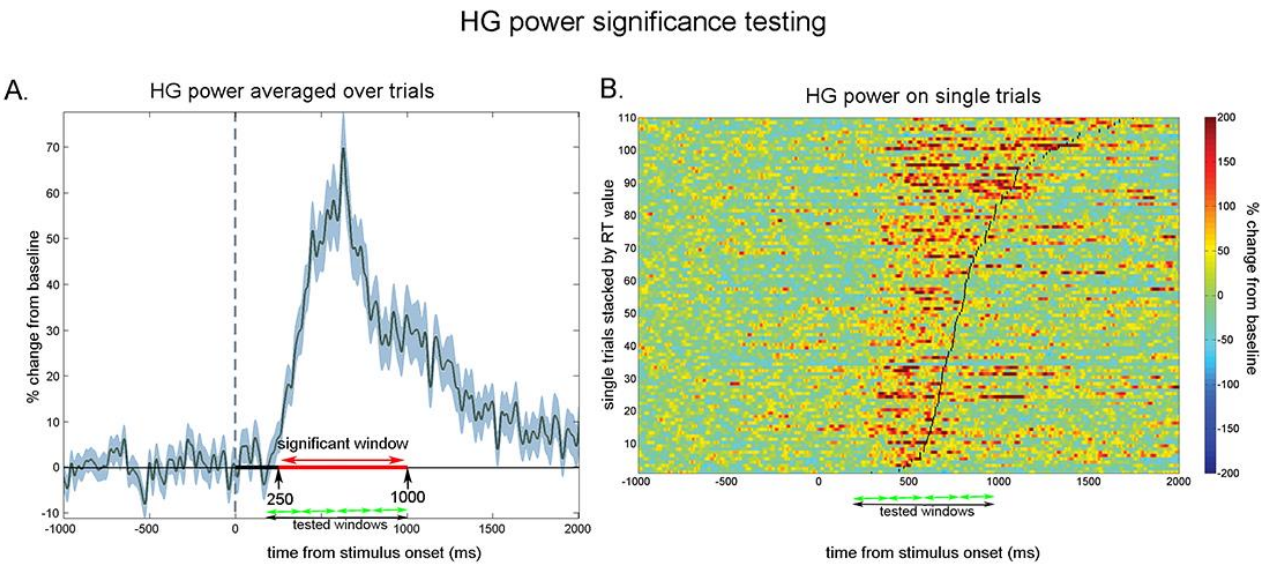

Figure S3: HFB power significance testing in each electrode. (A): The presence of HFB activity is first tested on the analytic amplitude of the HFB signal over trials in 1000-ms-long time-windows time-locked to the stimulus and to the response of 50-ms consecutive time-windows. The red line indicates the presence of significant HFB activity in this electrode. (B) HFB power in each trial is averaged over one to five 200-ms-long consecutive time-windows for each electrode with significant HFB stimulus and response-locked (green double arrows). The presence of HFB in almost every trial is visible here in warm colors. The number of time-windows included in the analysis for each electrode is determined by whether or not this electrode had significant HFB. Here, significant HFB was found from 250 to 1000 ms after stimulus onset. Therefore, mean HFB values are calculated for windows 2 to 5, going from 200 to 400 ms, 400 to 600 ms, 600 to 800 ms, and 800 to 1000 ms post-stimulus onset respectively.

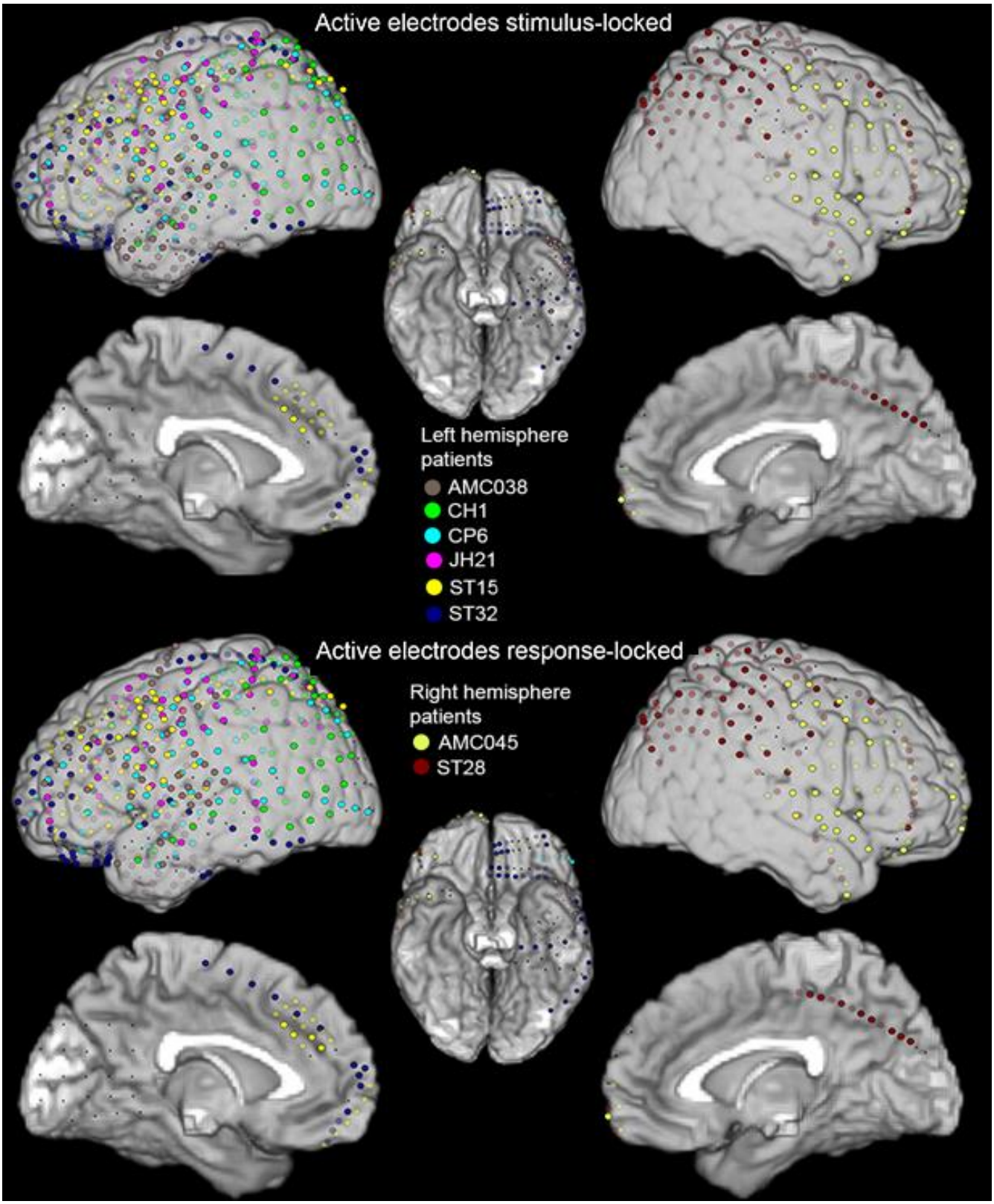

Figure S4: Active electrodes (i.e., with significant HFB, in bright colors) stimulus (A) and response-locked (B) for the 8 patients with analyzed ECoG data. Each color represents the electrodes for a different patient.

Electrodes with no significant HFB are shown with faded colors and bad electrodes (with artifacts, epileptic activity, or over resected tissue) are shown as black small dots.

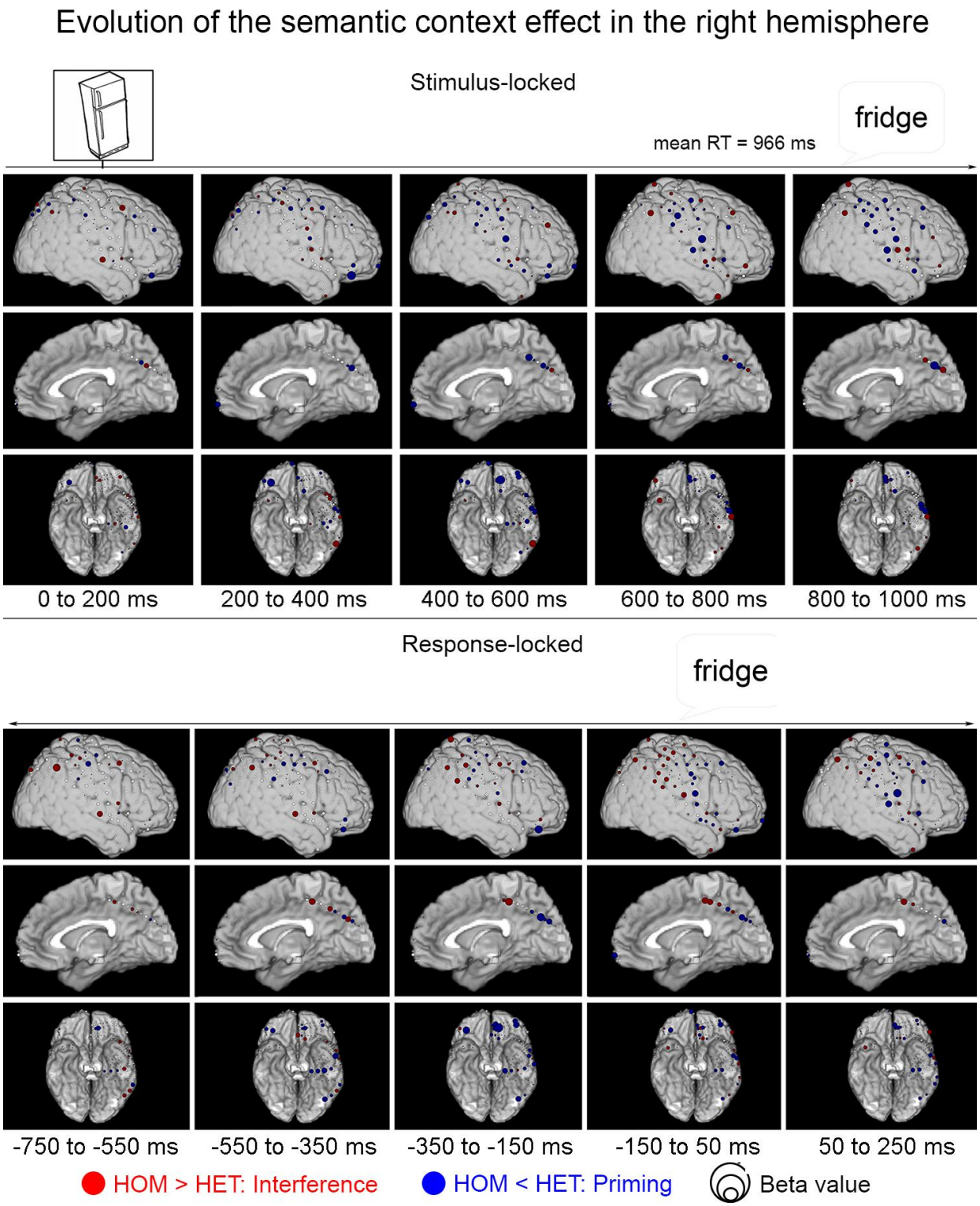

Figure S5: Evolution of the semantic context effect per recording site stimulus (A) and response-locked (B) on the right lateral, medial and ventral views of the MNI brain. Each column corresponds to one of 5 time-windows of analyses. Electrodes colored in red correspond to electrodes showing more HFB activity in HOM than HET blocks (in the direction of the semantic interference effect), electrodes colored in blue

correspond to electrodes showing more HFB in HET than HOM blocks (in the direction of semantic priming), as estimated with the linear mixed effect models ran for each electrode for visual purposes. The size of the dots is proportional to the raw β values for the main effect of semantic context.

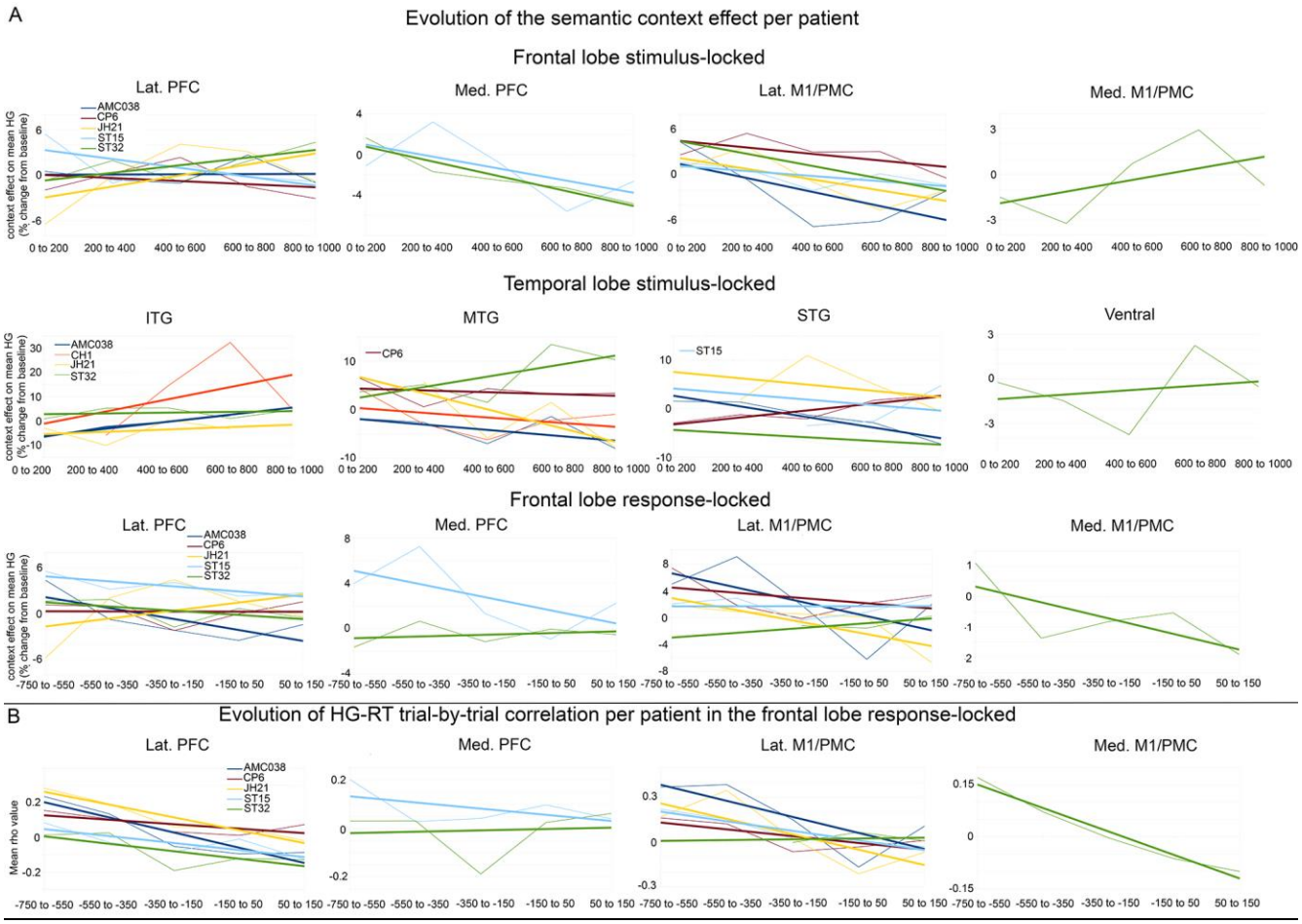

Figure S6: Evolution of the semantic context effect (A) and of the HFB-RT correlations (B) per patient and per structure for models with significant interactions between Semantic Context and Window and/or 3-way interactions between Semantic Context, Window, and Structure (in A); or a main effect of Window (in B). Each color corresponds to a different patient. Thin lines correspond to the mean values per time-window per patient and straight lines correspond to the linear regressions of the thin lines, indicating the overall slope of the effect per patient.

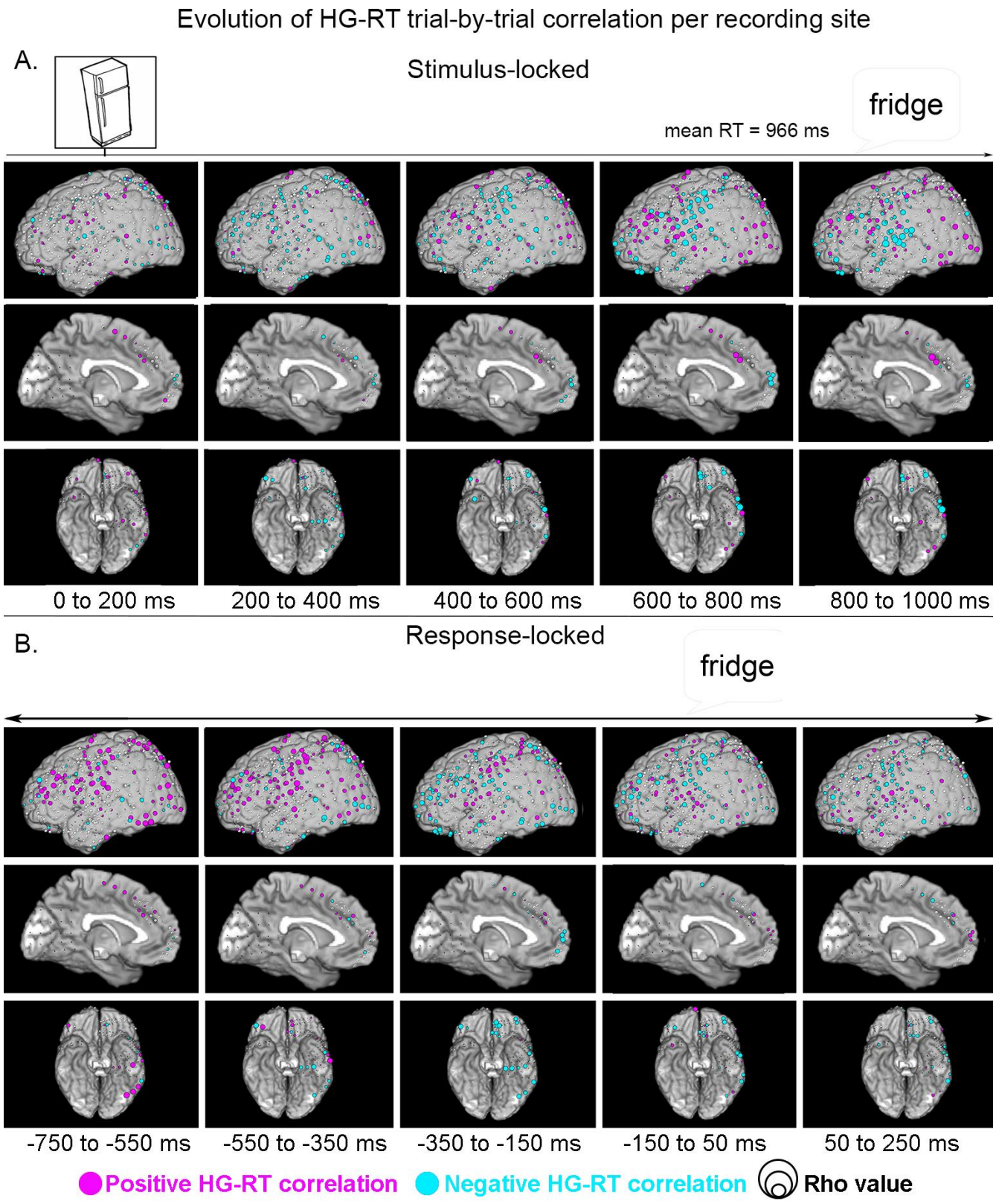

Figure S7: Evolution of the HFB-RT correlations per recording site stimulus (A) and response-locked (B) on the left lateral, medial and ventral views of the MNI brain. Each column corresponds to one of 5 time-

windows of analyses. Electrodes colored in pink correspond to electrodes showing positive HFB-RT correlations, meaning more HFB associated with longer RTs. Electrodes colored in aqua correspond to electrodes showing negative HFB-RT correlations, meaning more HFB associated with shorter RTs, as estimated with the Spearman rank correlation coefficient calculated for each electrode. The size of the dots is proportional to the ρ values.

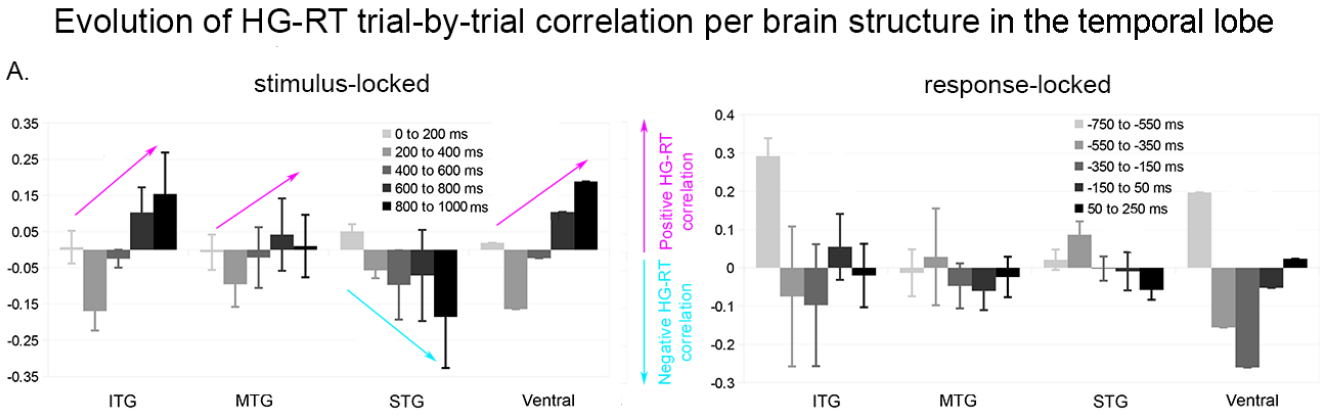

Figure S8: Evolution of the HFB-RT correlation coefficient per brain structure in the temporal lobe stimulus (A) and response-locked (B). Time-windows are color-coded in 5 shades of gray (from light to dark). Positive values correspond to positive HFB-RT correlations (more HFB associated with longer RTs), negative values correspond to negative HFB-RT correlations (more HFB associated with shorter RTs). Pink and aqua arrows indicate the direction of the HFB-RT correlation by Window interactions in each brain structure.

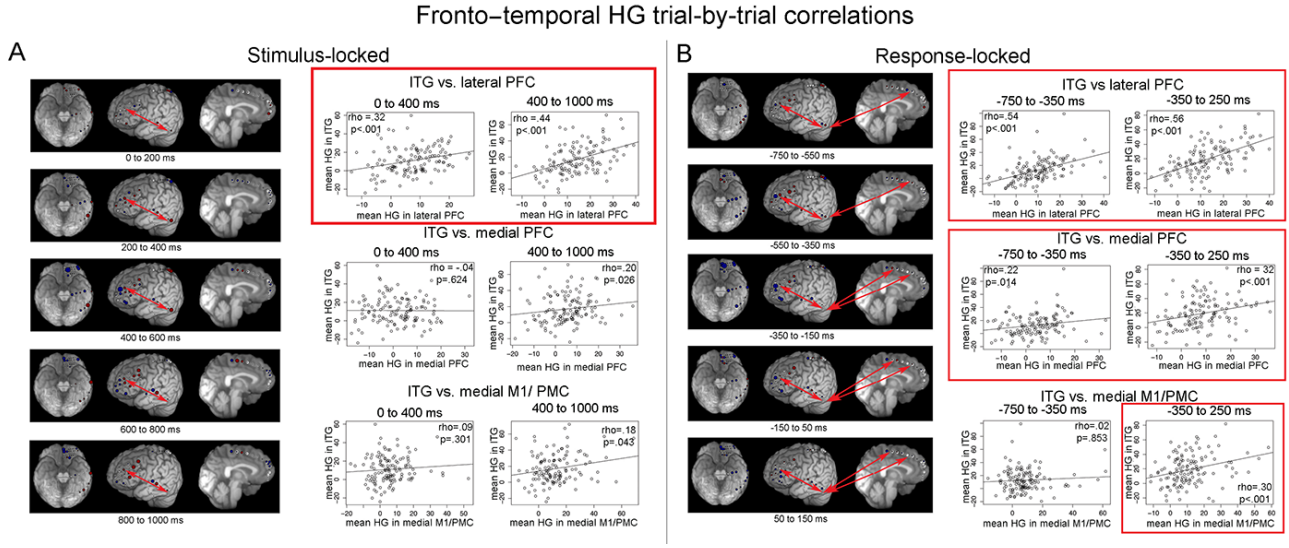

Figure S9: Correlations between within-trial mean HFB in the ITG and in lateral PFC, medial PFC, and medial M1/PMC, stimulus (A) and response-locked (B) between 0 and 400 ms and 400 to 1000 ms stimulus-locked, and between -750 and -350 ms, and -350 to 250 ms response-locked in patient ST32. In each plot, the correlation coefficient and associated p-value is indicated. Plots framed in red correspond to significant correlations. The brain plots to the left of the correlation plots correspond to the evolution of the semantic context effect in ST32. The red double-sided arrows on the brain plots indicate which regions showed significant trial-by-trial HFB correlations in which time-window.

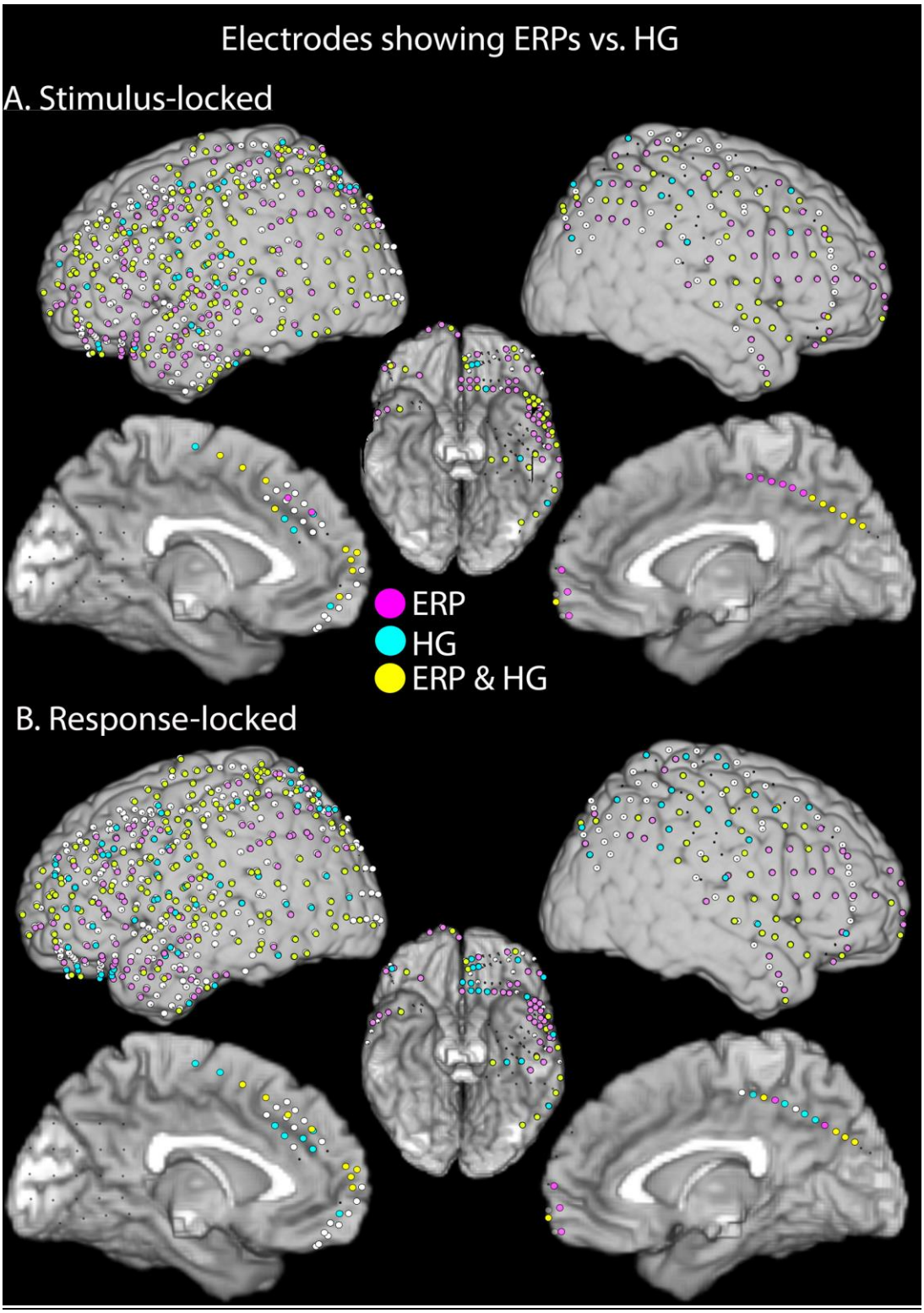

Figure S10: Electrodes showing significant ERPs vs. electrodes showing significant HFB in the stimulus (A) and response-locked (B) 1000-ms time-windows under analysis. The pink dots correspond to electrodes only showing ERPs, pink dots correspond to electrodes only showing HFB, and the yellow dots correspond

to electrodes showing both ERPs and HFB.